A STUDY OF THE INTERACTION LOSS OF PROTONS AND DEUTERONS IN NaI

By

MUNAWAR SULTANA AHMAD

B.Sc., University of Dhaka, 1974

M.Sc., University of Dhaka, 1975

A THESIS SUBMITTED IN PARTIAL FULFILMENT OF

THE REQUIREMENTS FOR THE DEGREE OF

MASTER OF SCIENCE

in

THE FACULTY OF GRADUATE STUDIES

DEPARTMENT OF PHYSICS

We accept this thesis as conforming

to the required standard

THE UNIVERSITY OF BRITISH COLUMBIA

JULY 1988

In presenting this thesis in partial fulfilment of the requirements for an advanced degree at the University of British Columbia, I agree that the Library shall make it freely available for reference and study. I further agree that permission for extensive copying of this thesis for scholarly purposes may be granted by the head of my department or by his or her representatives. It is understood that copying or publication of this thesis for financial gain shall not be allowed without my written permission.

Department of Physics

The University of British Columbia
1956 Main Mall
Vancouver, Canada
V6T 1Y3

Date 27th July '88

ABSTRACT

Interaction losses in sodium iodide crystals have been directly measured for protons in the range of energies from 139 to 444 MeV and for deuterons of 277 MeV. Calculations of the expected loss were made for protons over the range 151-500 MeV using the best currently available reaction cross section data. Our experimental values are typically about 21% lower than the calculated values.

The interaction loss for 277 MeV deuteron in NaI is about 8% lower than the calculated value obtained using the deuteron cross section value of Measday and Schneider. Using their calculated value of 100 MeV deuteron interaction loss as a reference point, we calculated the loss for 277 MeV deuterons and from a fit to our data we obtained the cross section for deuterons at an average energy of 188.4 MeV to be 2590 ± 180 mb, which is about 20% lower than the cross section obtained from the empirical relation that σ(d-A) is 2σ(p-A) at half the energy.

TABLE OF CONTENTS

LIST OF TABLES

LIST OF FIGURES

ACKNOWLEDGEMENTS

I would like to express my sincere gratitude and appreciation to my supervisor, Professor David F. Measday for his guidance, advice, patience and encouragement throughout this work.

I would like to thank Dr. Martin Salomon, Dr. Dezsö Horváth, Dr. Shirvel Stanislaus and Tony Noble for their assistance in the preparation and running of the experiments. Dr. Stanislaus is also thanked for many helpful suggestions during the course of this work.

I am indebted to Dr. Dave Hutcheon, without whose expertise and patience we would not have found the deuterons in the first place.

The advice and assistance of Dr. J.L. Beveridge and Dr. Alan Fry during my first few months at TRIUMF are also thankfully acknowledged. Thanks are due to Mrs. Rani Theeparajah for her careful typing of the thesis.

Finally, I wish to thank my husband, Salahuddin for his support and enthusiasm for education, and also both my parents and parents-in-law for their continuous encouragement.

DEDICATION

TO

MONJULI

CHAPTER 1

Introduction

When a charged particle passes through a material it can undergo nuclear interactions. In many nuclear physics experiments it is important to know the number of these interactions. These experiments are basically of two types. In the first type a counter is used to measure the kinetic energy of the charged particle by stopping it in a material such as plastic scintillator, silicon, germanium or sodium iodide. In the second type, to reduce the incoming energy of the charged particle or to stop it as in a range measurement, materials such as aluminum, carbon or copper are used.

For total-energy counters only nuclear inelastic interactions are important. Elastic scattering is peaked forward, and the particle normally stays within the confines of the sensitive volume. In an elastic collision the energy transfer to the nucleus is small and for most cases only a few percent of the energy transfer is more than 2% of the incoming energy [1]. The energy which is transferred to the nucleus due to an elastic collision may not be detected by the counter, but the elastically scattered particles will not be distinguished from those which have not undergone nuclear interaction because of the finite resolution of the counter. Typically the resolution of the counter is 1 to 2% for 350 MeV proton energy.

In an inelastic interaction, energy is lost for several reasons:

a) the negative Q-value of the reactions

b) the production of uncharged particles such as neutrons and gamma rays which do not deposit their energy in the crystal

c) the production of heavier charged particles such as tritons, alphas etc for which the scintillator response will be non-linear.

One way or other, energy will be lost and the energy deposited in the counter will be less than that for protons which do not interact. Thus for the total energy stopping counters the proton can be considered as lost from the full energy peak if it undergoes a nuclear inelastic interaction.

Such corrections have been considered by several authors [2-5] who have emphasized energies up to 150 MeV.

1.1 Inelastic nuclear reaction cross-sections

Reaction cross sections, defined as total minus total elastic cross sections for nucleons incident on a nucleus, are one of the basic properties needed for an understanding of the nuclear strong interactions. To describe the nucleon-nucleus interaction in terms of the multiparameter optical model potential, one needs experimental information on total cross sections, reaction cross sections, differential elastic scattering cross sections and polarizations [6-11]. The reaction cross-section is particularly important for limiting the range of the imaginary part of the optical model potential.

The nucleon-nucleus interaction can also be described within the

framework of a semi classical approximation which relates the reaction cross sections to the transparency of the nucleus which is defined as the difference from unity of the ratio of the reaction cross section to the geometrical cross section. The reaction cross sections can be calculated from a theory based on a simplified model where one considers the nucleon-nucleus interaction as a sum of nucleon-nucleon interactions. Here the nucleus is considered as a degenerate Fermi gas of nucleons in a nuclear potential of radius $R = r_o A^{1/3}$. The reaction cross-sections is

$$\sigma_R = \pi R^2 (1-T) \tag{1.1}$$

where

$$T = \frac{1 - (1 + 2KR)e^{-2KR}}{2K^2R^2} \tag{1.2}$$

is the transparency of the nucleus. K is the absorption coefficient which characterizes the absorptive property of the potential and is a function of the cross section for nucleon-nucleon scattering, and thus is energy dependent. If the Coulomb repulsion in compound nucleus formation is considered [12], the modified formula for the reaction cross section is

$$\sigma_R = \pi(r_o A^{1/3} + \lambda\!\!\!^{-})^2 \left[1 - \frac{Zze^2}{(R+\lambda)E_o}\right][1-T] \tag{1.3}$$

where E_o is the incident proton energy and $\lambda\!\!\!^{-}$ is the reduced wavelength of the incident particle.

The total reaction cross-sections for protons on various nuclei have

been measured by many experimenters. Pollock and Schrank [13] have shown that around 200 MeV, in the region where the reaction cross-section varies only slightly with energy, the cross-section can be fitted to the following relation

$$\sigma_R \ (fm^2) \ = \ (\pi r_o^2 A^{2/3} - 5.0) \qquad (1.4)$$

where r_o = 1.26fm, and so $\pi r_o^2 \approx 5.0 fm^2$. Thus it was possible to make precise interpolations for reaction cross-section of elements for which few or no data were available. There is a clear minimum of the proton reaction cross-section around 250 MeV for most of the elements. Above this energy the onset of pion production causes a slight increase of the cross section up to 600 MeV. Above 600 MeV the data are few and not sufficiently reliable to give information on the high-energy behaviour. However, there are indications that σ_R reaches a maximum around 2 GeV and then decreases very slightly at higher energies [14,15]. Due to the large errors on the measurements in this energy, Measday and Richard-Serre [1] chose to assume a constant value for the reaction cross section for energies greater than 250 MeV.

Renberg et al. [16] fitted their experimental data on reaction cross section (up to 567 MeV incident proton energy on NaI) with a theoretical curve (eq. 1.3) which provided the best values for r_o and K and hence nuclear transparencies of some of the elements could be calculated. The transparency was seen to decrease with increasing mass number which implies that the reaction cross section comes closer and closer to the geometrical cross section.

Measday and Richard-Serre [1] calculated the number of nuclear

inelastic interactions of stopping protons in various materials using the then known reaction cross sections. The calculation proceeded by a simple step integration method. The range of the proton in that particular material was divided into n number of cells of equal length (~0.1 g/cm^2). The total fraction of interactions is then given by

$$f = 1 - \exp\left(-\sum_i n_i \sigma_i\right) \qquad (1.5)$$

where n_i is the number of atoms/cm^2 in the ith cell and σ_i is the average cross section in that cell. Since the cross section is energy dependent, it was necessary to determine the average energy of the proton in each cell. The energy at the end of the first cell was calculated using the range-energy programme [17]. The average energy of the proton in that cell was found, and the corresponding reaction cross section was interpolated from the then available data. Thus the number of interactions in the first cell was determined. The integration continued until 10 MeV, at which energy the reaction cross section for all elements except carbon is assumed to be zero. This cut-off at 10 MeV was used because all experimental determinations of the number of interactions in total energy counters must define the non-interacting peak, and a cut at 10 MeV below the maximum of the peak had proved a reasonable compromise for protons. For range measurements this corresponds to an uncertainty in the peak of ~0.1 g/cm^2 for light elements and 0.2 g/cm^2 for heavier elements. A 10 MeV proton, any way, cannot penetrate the Coulomb barrier of most nuclides.

1.2 Motivation of the present work

In many nuclear physics scattering experiments charged particles appear in the outgoing channel and detectors are used to detect their full energy. It is convenient to use pulse height in sodium iodide to specify the scattered particles. Since the pulse height will be smaller for a particle which has undergone a nuclear interaction, it is necessary to make a correction for particles lost from the full energy peak. This correction has been measured experimentally and/or calculated by several authors using available data on total reaction cross section which had been calculated [3,12], or measured by different groups [2,3,16,18-21]. A few studies have been made to determine the reaction probability for protons on sodium iodide crystal as a function of incident energy. Johnson et al. [22] were some of the first, and they measured proton interaction percentages at energies up to 68 MeV on sodium iodide with an overall accuracy of 10%.

Measday [4] measured and calculated the percentage of protons undergoing nuclear inelastic interactions for energies up to 160 MeV. The calculations were performed using an estimated cross section value from the plot of the energy dependent cross section against atomic number given by Johansson et al. [23]. The measured values have 4-10% inaccuracy. Palmieri and Wolfe [24] measured this loss for protons of up to 150 MeV energy on sodium iodide with a 20% accuracy. Measday and Serre [1] have summarized all experimental reaction percentage information available and using the then latest total reaction cross section information have calculated reaction percentages for protons stopping in

various materials including sodium iodide over the range 30-800 MeV with an overall accuracy of 5-10%.

Sourkes et al. [25] undertook the interaction loss measurements on sodium iodide in the energy range 50-150 MeV with an overall error of about 3%, while Goulding and Rogers [26] have measured this loss of protons of up to 150 MeV with 2-3% accuracy. Goulding et al. also calculated this percentage loss for 40-240 MeV protons and their values are slightly larger than those calculated by Measday and Serre [1].

Cameron et al. [27] and Bracco et al. [28] measured the efficiency of sodium iodide counter for detecting intermediate energy protons; Cameron et al. up to 150 MeV protons and Bracco et al. up to 350 MeV protons. The efficiency of a counter telescope was defined as I/I_o where I_o is the total number of protons incident on a counter telescope and I is the number of tagged protons which resulted in a full energy signal in the sodium iodide detector. An estimation of the interaction loss could be obtained from their data which is the ratio of $(I_o-I)/I_o$.

Renberg et al. [16] measured proton reaction cross sections for several elements and compounds, including sodium iodide for protons of energy 220-570 MeV with an error of 3%, which was a factor of three better than existing measurements in that energy region. Because of this error, the calculated values of the proton interaction probability become more uncertain and less dependable as the energy increases.

To obtain experimental values of the interaction loss for the protons on sodium iodide for energies beyond 150 MeV where few experimental data are available, and above 350 MeV where no experimental data are available, we have undertaken the measurements of proton undergoing

nuclear inelastic interactions in NaI for the energy range of 139-444 MeV using the TRIUMF cyclotron facility.

For heavier particles, the calculated and experimental data for the interaction loss are very few. Measday and Schneider [5] calculated this loss for deuteron and alpha particles of up to 160 MeV for sodium iodide and plastic scintillators while Bojowald et al. [29] calculated it for deuterons of up to 450 MeV in germanium, which are in good agreement with the only available experimental result of Eisberg et al. [30] who measured this loss for deuterons of up to 250 MeV on germanium.

Recently N.V. Sen et al. studied the elastic scattering of polarized deuterons from calcium and nickel [31] and oxygen [32] at intermediate energies. The data were analyzed in terms of the optical model and the reaction cross sections deduced were compared to predictions from the Glauber theory optical limit.

Watanabe [33] used the WKB method to calculate the angular distribution and the polarization of 94 MeV deuterons by carbon. The result of his calculation using well parameters which fit the scattering data of 40 MeV protons by carbon, was in good agreement with the measured values of the differential cross section. This suggests the empirical relation that cross section for deuteron in nuclei is twice the cross section for proton at half the energy.

CHAPTER 2

The Experiment

The aim of the present experiment was to study the interaction loss of protons and deuterons in sodium iodide crystals. The first experiment was performed in September 1986 when we used the proton beam, elastically scattered off a hydrogen target, to study the interaction loss. The final data taking was done in March '87 when direct beams of protons and deuterons were used. The experiment was performed using the polarized proton beam provided by the 1B primary beam line (BL1B) at TRIUMF.

2.1 Beam line 1B

The experiment was performed at the 1BT1 location of the TRIUMF cyclotron facility. The cyclotron accelerates negatively charged hydrogen ions and a proton beam is extracted by removing both electrons from the ions by inserting a stripper foil in the machine. The energy of the beam is variable up to a maximum of 520 MeV depending on the radial distance of the foil in the cyclotron. The beam is produced in 5 ns bunches with a time separation of 43 ns corresponding to the 23.055 MHz cyclotron radio frequency (RF). Two beams are typically extracted, one into the proton hall, the other into the meson hall (Fig. 2.1).

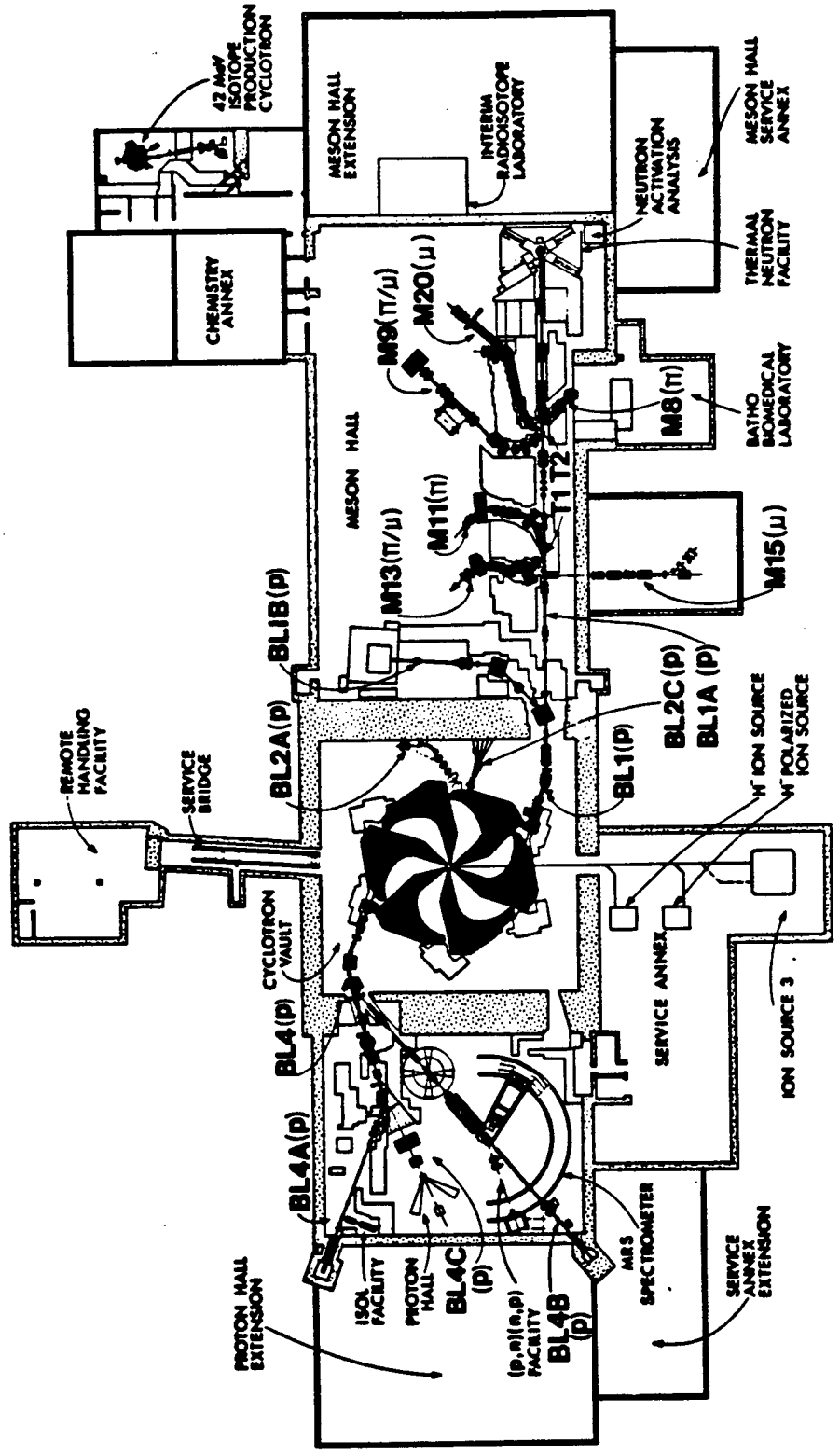

Fig. 2.1: TRIUMF beam lines and experimental facilities

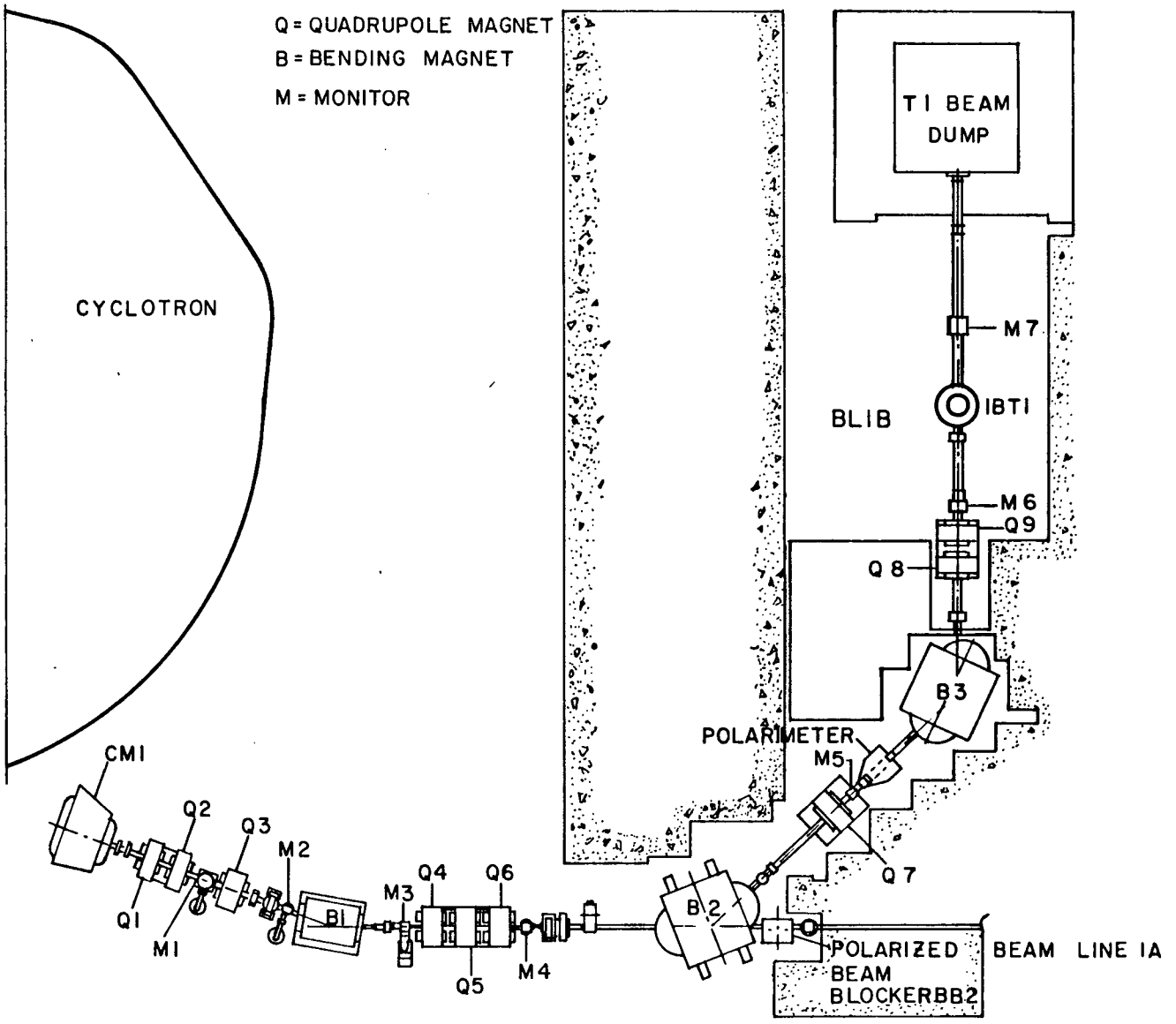

Fig. 2.2: Layout of beam line 1B

The schematic of the primary proton beamline 1B is shown in Fig. 2.2. Using magnetic elements (dipole, quadrupole magnets) as shown in Fig. 2.2, the proton beam from the cyclotron was transported to the experimental zone (1BT1) where the target and the detectors were mounted. In our September 86 measurement, a liquid hydrogen target was used while in the March 87 measurement a direct proton beam was used. A secondary deuteron beam was also produced during the March 87 run.

2.2 Production of the secondary deuteron beam

In order to measure the deuteron reaction losses in NaI crystal, a low intensity deuteron beam was produced for the first time on beam line 1B during the present experiment. The deuterons were produced from the primary proton beam using the reaction $p+p \rightarrow d+\pi^+$. The deuterons selected were those emitted at or very close to the primary beam direction, yielding ~292 MeV deuterons from a beam of 446 MeV protons.

The deuteron momentum is thus 6% higher than that of the primary beam, making it possible to suppress the background of scattered protons using the magnetic elements shown in Fig. 2.2. The production target was a 55 mg/cm^2 thick polyethylene (CH_2) foil in the beam line 1 vault section, just in front of the bending magnet 1BVB2 (or more simply B2, as in Fig. 2.2).

The magnetic field of B2 was set to deflect the primary beam 3 cm to the left of center onto a lead brick which served as a beam-stop, and which occupied the left-most 35% of the 10 cm diameter beam pipe.

Quadrupoles upstream of B2 produced a horizontal focus at the beam-stop; thus the particles getting past to the right of the beam stop were deuterons or elastically scattered protons from the CH_2 target, and possibly halo from the primary beam. The final bending magnet B3 was set to transport the deuterons of interest and to overbend any protons. Quadrupole magnets Q7, Q8 and Q9 were set to produce an achromatic double focus from the CH_2 target to the target location 1BT1.

The quadrupole and dipole MUX (Multiplex current read back) values and their direction of focus are given in Table 2.1. Beam in the cyclotron tank, which is not stripped and extracted, is accelerated to the outer edge of the tank where it slips out of phase with the RF, is decelerated back to the stripper foil and extracted. These protons arrive at the experiment at a different time.

A high energy probe can be used to intercept beam going past the stripping foil. In our experiment a wide foil (C type) heavily shadowed by an high energy probe was used.

2.3 NaI crystals (TINA and MINA)

In this experiment, the interaction loss of protons and deuterons in NaI were studied using TINA and MINA. TINA, which stands for TRIUMF Iodide of Natrium, measures 46 cm in diameter and 51 cm in length and is optically a single unit, viewed by seven phototubes. MINA, which stands for Montreal Iodide of Natrium measures 36 cm in diameter and 36 cm in length and is also an optically single unit viewed by seven phototubes.

Table 2.1

The beamline quadrupole values and their direction of focus for the deuteron beam (446 MeV protons and 292 MeV deuterons)

Quads	MUX Settings	Direction
Q1	213.6	H
Q2	304.0	V
Q3	341.8	H
Q4	39.6	V
Q5	183.8	H
Q6	139.9	V
Q7	127.2	H
Q8	242	V
Q9	272	H
1BVB2	559.8	
1BB3	570.6	

Both crystals are shrouded by large iron walls with opening apertures of 30 cm ϕ and 25 cm ϕ respectively. They are of excellent quality and such detectors are preferred for γ-ray detection when 100% efficiency and reasonable resolution are important characteristics of an experiment. TINA and MINA have been used in many different experiments [34-39] including studies in atomic and nuclear physics, but the best known work has been in particle physics experiments on the weak interactions where several key measurements [40-45] have been made. TINA and MINA have not been used for the detection of protons or deuterons before, although other NaI crystals have been often used in a variety of experiments especially by the Alberta group [46].

2.4 Experimental arrangement

A schematic of the experimental setup for the '86 and the '87 runs is shown in Figs. 2.3 and 2.4 respectively. We shall first discuss the experimental details of the '86 run and then the '87 run.

In the '86 run, we used a liquid hydrogen target which was contained in a cylindrical target flask of 5 cm diameter and 5 cm length. This was chosen in such a way that a reasonable event rate was obtained with minimum energy loss of the incoming protons. The target flask was made of 0.13 mm kapton and was placed inside an evacuated scattering chamber which had a kapton window. The elastically scattered proton beams from the p+p→p+p reaction were detected by the two large NaI detectors TINA and MINA (discussed in Section 2.3). Two plastic scintillators

which covered the faces of TINA and MINA were used to identify charged particles. A small plastic scintillator (1" x 1" x $^1/_{16}$") was used in front of TINA in order to define the angle. TINA and MINA were placed at different angular positions with respect to the incoming proton beam and at equal distances from the target (~1.25 m).

For a known energy incident proton beam hitting the liquid hydrogen target, the energies of the elastically scattered and recoiling protons detected by TINA and MINA at different angular positions could be known using the TRIUMF kinematic handbook [47] and the computer programme TRIUMF KIN2BODY. The actual energies of protons detected by TINA and MINA were slightly lower than the theoretical values given by the handbook or KIN2BODY programme because of the energy loss in the target vessel, plastic scintillators, iron, and aluminum layers in the front faces of TINA and MINA.

The incident proton energies and the energies of the scattered protons detected by TINA and MINA at different angular positions (calculated using TRIUMF computer programme LOSS) are summarized in Table 2.2. The primary energy of the proton beam was determined from the cyclotron stripper parameters and is accurate to about 1 MeV.

In the '87 run as shown in Fig. 2.4, two multiwire gas proportional chambers (MWPC) separated by 0.45 m were mounted immediately after the evacuated beam pipe window (.02 mm stainless steel) to measure the particle trajectories. The multiwire proportional chambers had four outputs (X_L, X_R, Y_L, Y_R) and had a delay line readout system which gave about 0.5 mm resolution in the horizontal and 2 mm resolution in the vertical. Following the wire chambers was a lead and steel collimator

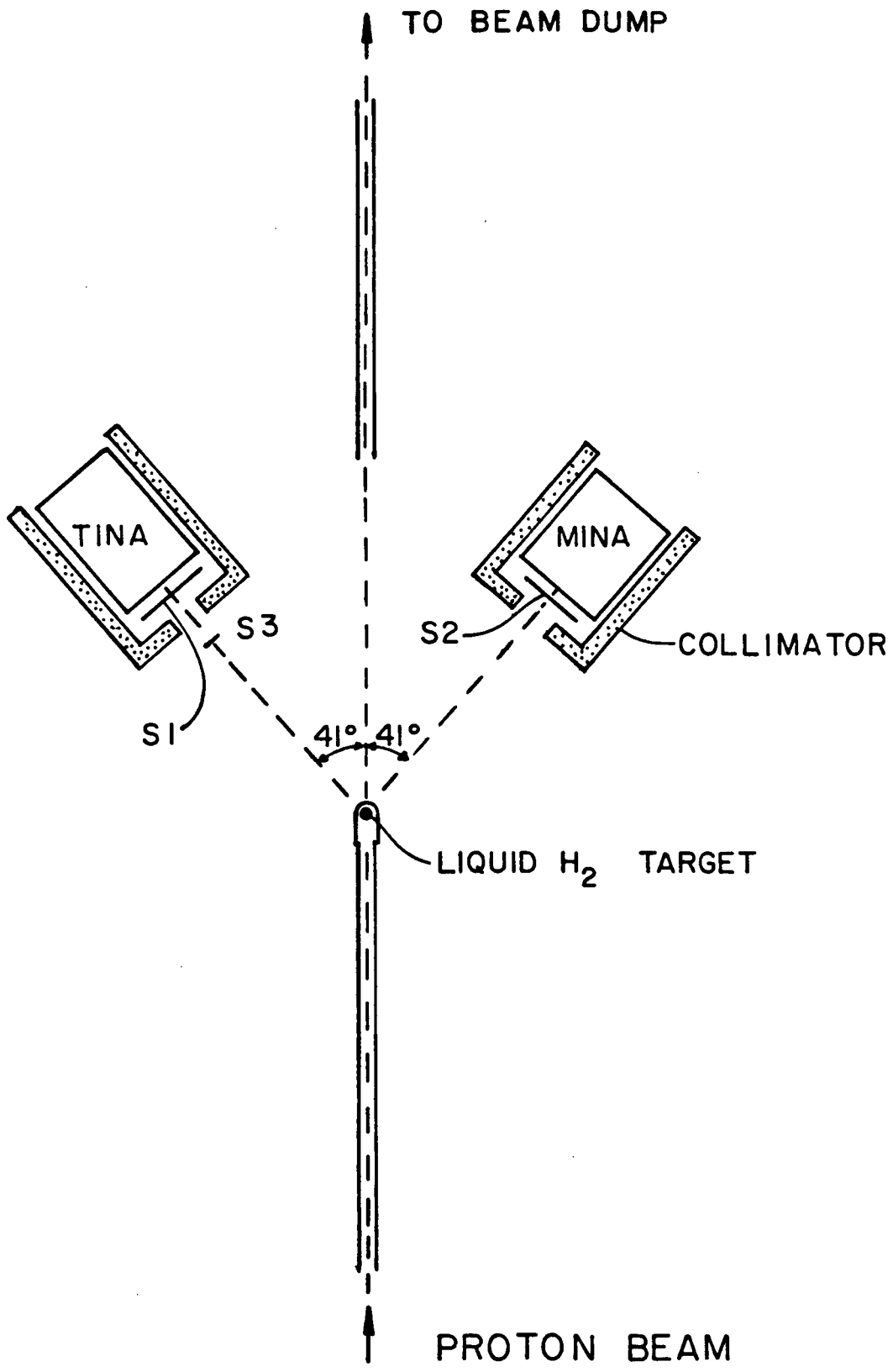

Fig. 2.3: Schematic of the experimental setup (1986 run)

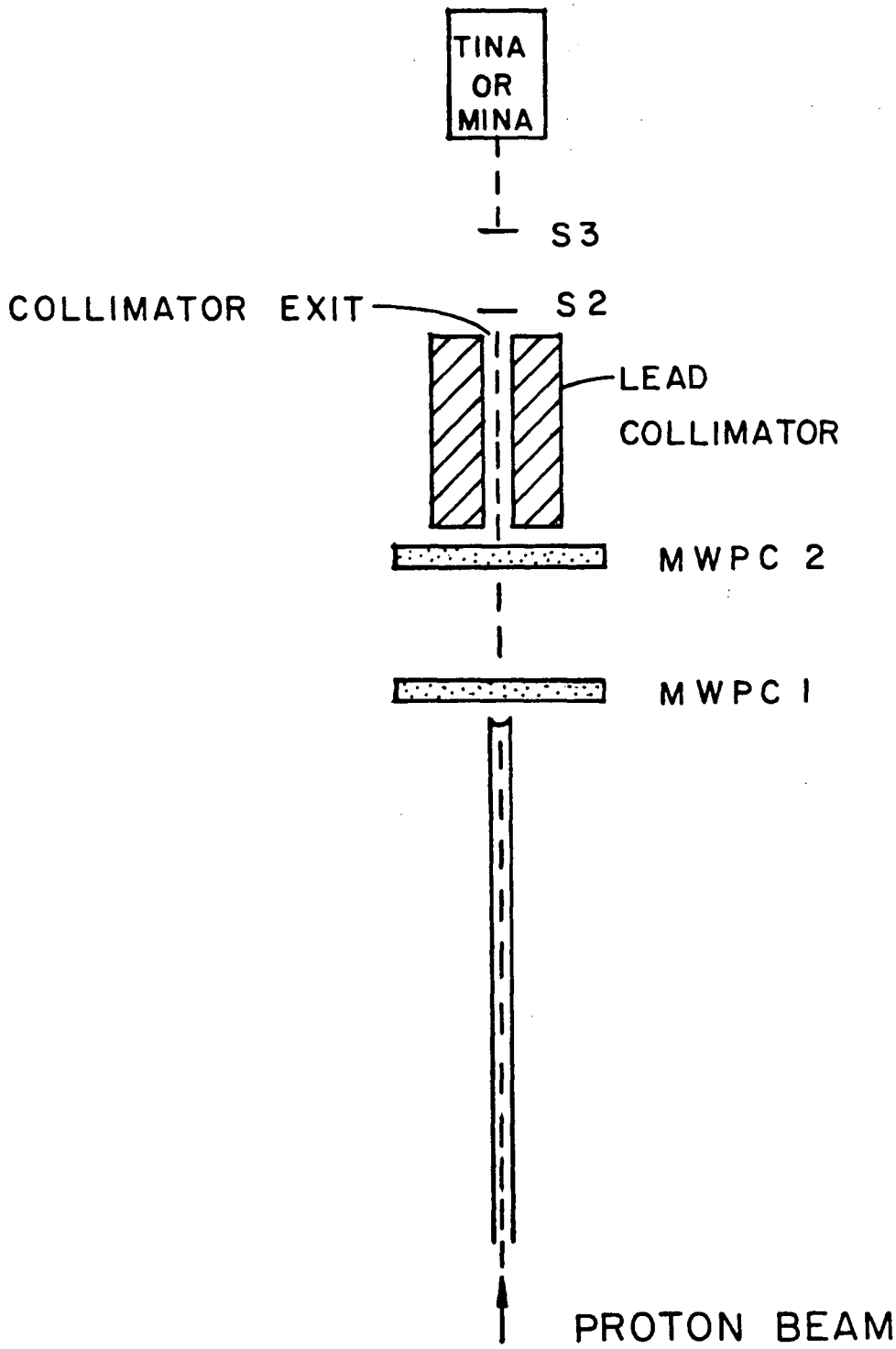

Fig. 2.4: Schematic of the experimental setup (1987 run)

Table 2.2

Proton energies in TINA and MINA

Incident proton beam energy (MeV)	Angular position of TINA with respect to incident beam θ_T	Theoretical proton beam energy in TINA (MeV)	Actual proton beam energy after energy loss correction in TINA (MeV)	Angular position of MINA with respect to incident beam θ_M	Theoretical proton beam energy in MINA (MeV)	Actual proton beam energy after energy loss correction in MINA (MeV)
497	41°	254.1	249.3	42°	242.9	235.8
497	47°	202.5	196.9	36.5°	294.5	288.2
497	54°	146.3	139.3	30°	350.7	344.9
451	41°	232.8	227.7	43°	218.2	210.6
403	41°	210.1	204.7	43.5°	192.9	184.7

having an opening of 51 mm diameter. The collimators were of sufficient thickness to stop any of the particles from the primary or secondary beams. A plastic scintillator S_2 was mounted immediately after the collimator and about 1.25 m beyond it a second plastic scintillator S_3 was mounted in front of the NaI crystal (TINA and MINA). The first part of the '87 run was with the deuteron beam and for this S_3 and MINA were used. For the second part we studied the reaction loss with the direct proton beam and for this S_3 and TINA were used. TINA or MINA were mounted in such a way that the beam could hit directly the front face of it, i.e. the angular position of TINA or MINA with respect to incident beam was 0°. The dimension of these scintillators and the MWPCs are given in Table 2.3. The energies of the proton and the deuteron beam are given in Table 2.4.

For a 446 MeV proton beam which yields about 291.6 MeV deuterons, beamline quadrupoles were set to the optimum tune condition. In fact quads 7, 8 and 9 were set to transport deuterons from the production target to an achromatic horizontal and vertical focus at 1BT1.

During the '87 run, the direct beam was used after the deuteron measurement. Because it was very difficult to remove the polyethylene target from the vault section at that moment, it was left there for the rest of the experiment but the 8" lead beam stopper was removed. The dipole and quadrupole magnets were reset for protons.

Table 2.3

Dimension of scintillators and MWPCs used in the '87 run

Counters	Dimension
MWPC 1	5" x 5"
MWPC 2	5" x 5"
S2	1 1/4"ϕ x 1/16"
S3 (TINA)	1" x 1 1/2" x 1/32"
S3 (MINA)	8" x 8" x 1/8"

Table 2.4

Energies of the proton and the deuteron beam ('87 run)

Particle	Incoming energy in MeV	Energy detected in NaI crystal after energy loss correction* in MeV
p	446	443.9
	348	345.7
d	291.6	276.8

* Energy loss in plastic scintillators, aluminum and iron layer in TINA and MINA were incorporated. For protons, additional energy loss in the deuteron production target CH_2 was also incorporated.

2.5 Electronics and data acquisition

A schematic of the electronics used in the '86 run is shown in Fig. 2.5. In this diagram the squares labelled D, D1, CFD represent discriminators. Linear signals above a threshold (set by user) are converted into logic signals by the discriminators. CFDs (constant fraction discriminators) are used where the timing information is important because for these CFDs the timing of the output pulse is relatively independent of the size of the pulse. The triangles represent linear or logic fan-in/fan-out units. The triangles with arrows represent attenuators and the circles give the CAMAC locations of ADC's, scalers, bit registers etc. which were read by the computer. Data were accumulated in two modes. First with full target and then with empty target to subtract the background.

The cyclotron radio frequency signal, usually known as the RF signal, was transmitted directly from the main control room to the M9 counting room where the data acquisition electronics and the PDP11/34 computer were located to record the data on magnetic tape for each event.

Seven signals each from TINA (T1, T2....T7) and MINA (M1, M2....M7) and three signals from scintillators mounted in front of TINA (T_A, T_B and T_C) and one signal from the scintillator mounted in front of MINA (M_A) for charged coincidences were transmitted from the experimental area to the counting room. Signals T_A and T_B were from scintillator S_1 and T_C was from S_3, the very small scintillator which was placed in front of TINA to define the angle of the proton into TINA.

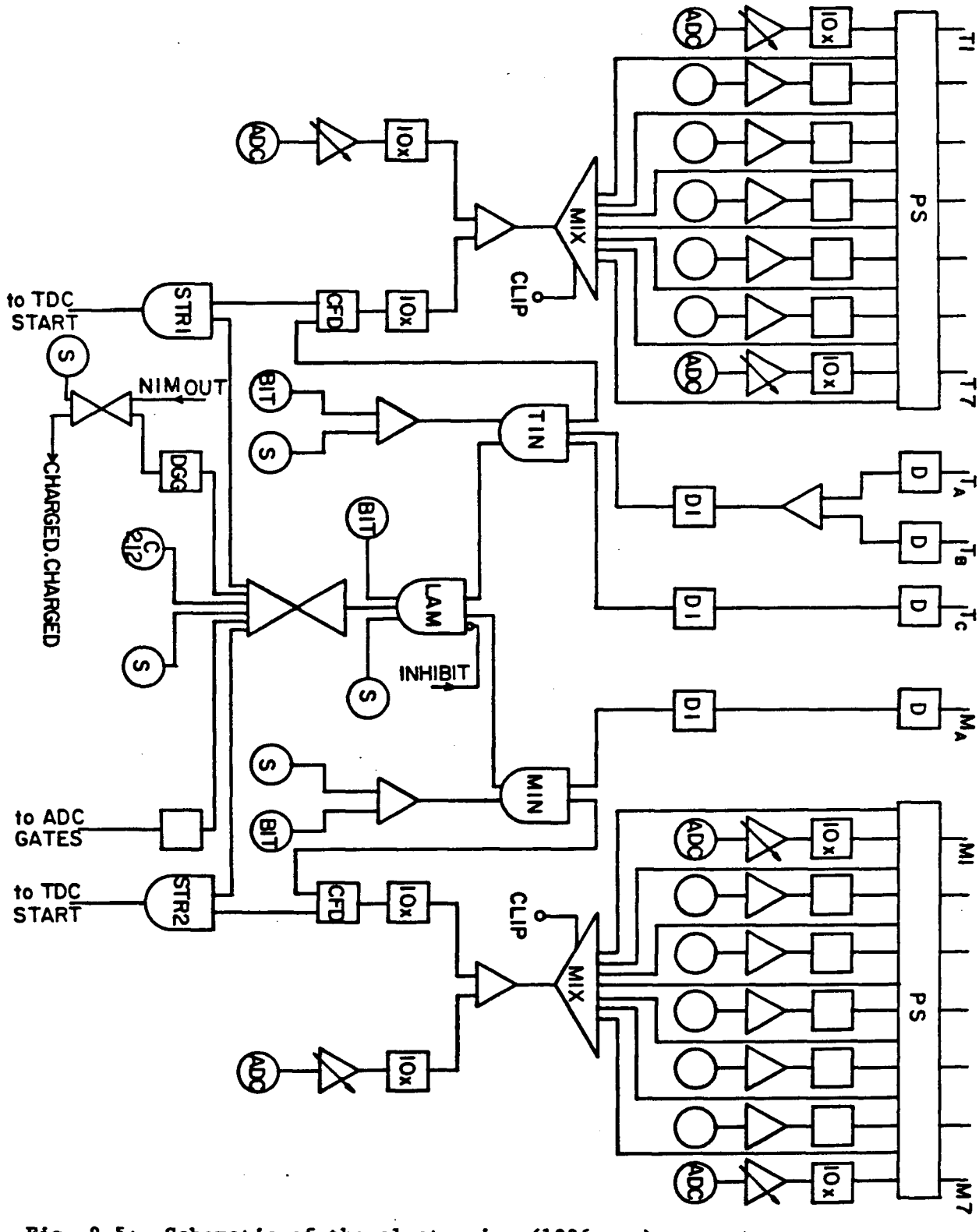

Fig. 2.5: Schematic of the electronics (1986 run)

In this experiment, the phototube signals from TINA and MINA (seven each) were split into two parts by a passive splitter (PS). The larger parts (~80% by amplitude) were amplified six times with the help of amplifier (LRS 612A) and attenuator combinations and were fed into twelve input, high resolution CAMAC Analogue to Digital Converters (ADC-LRS 2258A). Signals from the seven smaller parts (~20% by amplitude) were sent to a mixer (MIX) to get a summed output signal. A clipped signal from the mixer was obtained and a quad linear fan in/fan out (LRS428F) was used to fan out this signal in two parts.

The first part was amplified using an amplifier (LRS612A) and then was fed into CAMAC ADCs. The second part after amplification was sent to a constant fraction discrimator (CFD-ORTEC 934).

Signals from scintillators T_A and T_B were sent to a quad discriminator (LRS 821Z) from which NIM level outputs were obtained. Signals T_A and T_B were then fed into a logic fan in/fan out unit (LRS429A) the output of which was sent to discrimator DI (LRS621BLZ). A signal from T_C was also sent through a discriminator; the two discriminator outputs and a logical output from the CFD were then fed into triple 4-fold logic coincidence unit (TIN-LRS465). Timing of these three signals were adjusted in such a way that there was clear overlap (coincidence) between all three. Similarly timing of the discriminator signal from M_A was adjusted so that there was an overlap between this and the CFD signal coming to the coincidence unit (MIN). Two signals from TIN and MIN via a fan out unit were sent to a bit register and a visual scaler. Another output was sent to the coincidence unit known as LAM (Look At Me) and the coincidence output was sent to fan out unit (LRS429A).

Several outputs were used from this unit. The widths of these outputs were adjusted by sending these signals to discriminators. One output was used as a C212 strobe. Two outputs were stretched to 500 ns and used as gates to the ADC. Two outputs were sent to coincidence units STR1 and STR2 where coincidences with CFD outputs from TINA and MINA were made. Output signals from STR1 and STR2 having TINA and MINA CFD timing respectively were used as TDC starts for two 2228A LeCroy Camac Octal Time to Digital Converter. An output was stretched to 1 ms by a Dual Gate Generator (DGG-LRS222) and was sent to a fan in unit, where a computer busy signal was also fed. An output of this unit was used as an inhibit signal to the coincidence unit known as LAM.

There were two types of data read onto tape. Type 1 events were the strobe events while type 2 events were just the scalers. The data acquisition system started with the LAM signal. ADC gates were set, and ADCs provided the energy information in each counter. TDC clocks were started by the TINA and MINA CFD signals and stopped by the RF signal and these are called RFT and RFM respectively. Thus these TDCs give the time of flight of the protons to TINA and MINA. One event was handled at a time. A 1 ms gate from the Dual Gate Generator was set which gave protection against events occurring immediately afterwards until the computer starts reading the CAMAC module information. Whenever a buffer was full the buffer was transferred to tape. If the computer was busy processing an event, the NIM driver sends an inhibit signal to the LAM coincidence unit to stop more events from piling up.

For a number of coincidences a bit was set in the C212 bit registers whenever a strobe fired. The purpose of this is that by examining the

bit pattern we could then reconstruct the event.

A schematic of the electronics used in the '87 run is shown in Fig. 2.6. The MINA (or TINA) signals were treated the same way as described in the '86 run.

Signals from S_2 and S_3 were delayed and sent to linear fan outs. An output from each of these was sent to ADCs, the other one to CFDs. One CFD output was sent to a coincidence unit ($S_2.S_3$ or Event). One of the outputs of the Event coincidence unit was sent to the coincidence unit LAM, that is, the event trigger was derived from a coincidence between the two plastic scintillators, with the time of the trigger being defined by the thick scintillator. The TDC clocks were started by the LAM signal and stopped by the RF signal.

In LAM, a new event was vetoed when there was an inhibit signal arising out of the computer busy and/or event busy from a preceding event. The output signal from LAM were logically fanned out by the Fan-out unit and the widths of each outputs were adjusted using discriminators, so that they had sufficient widths to be used as C212 strobes, ADC gates and TDC starts. The RF signal was sent to a discriminator and then to a TDC stop. Signals W_1 (X_L, X_R, Y_L, Y_R) and W_2 (X_L, X_R, Y_L, Y_R) from the delay line multiwire proportional chambers (W_1 and W_2) were delayed and were used as TDC stops.

In both experiments, the data were recorded event by event on a magnetic tape using the TRIUMF standard multi data acquisition system.

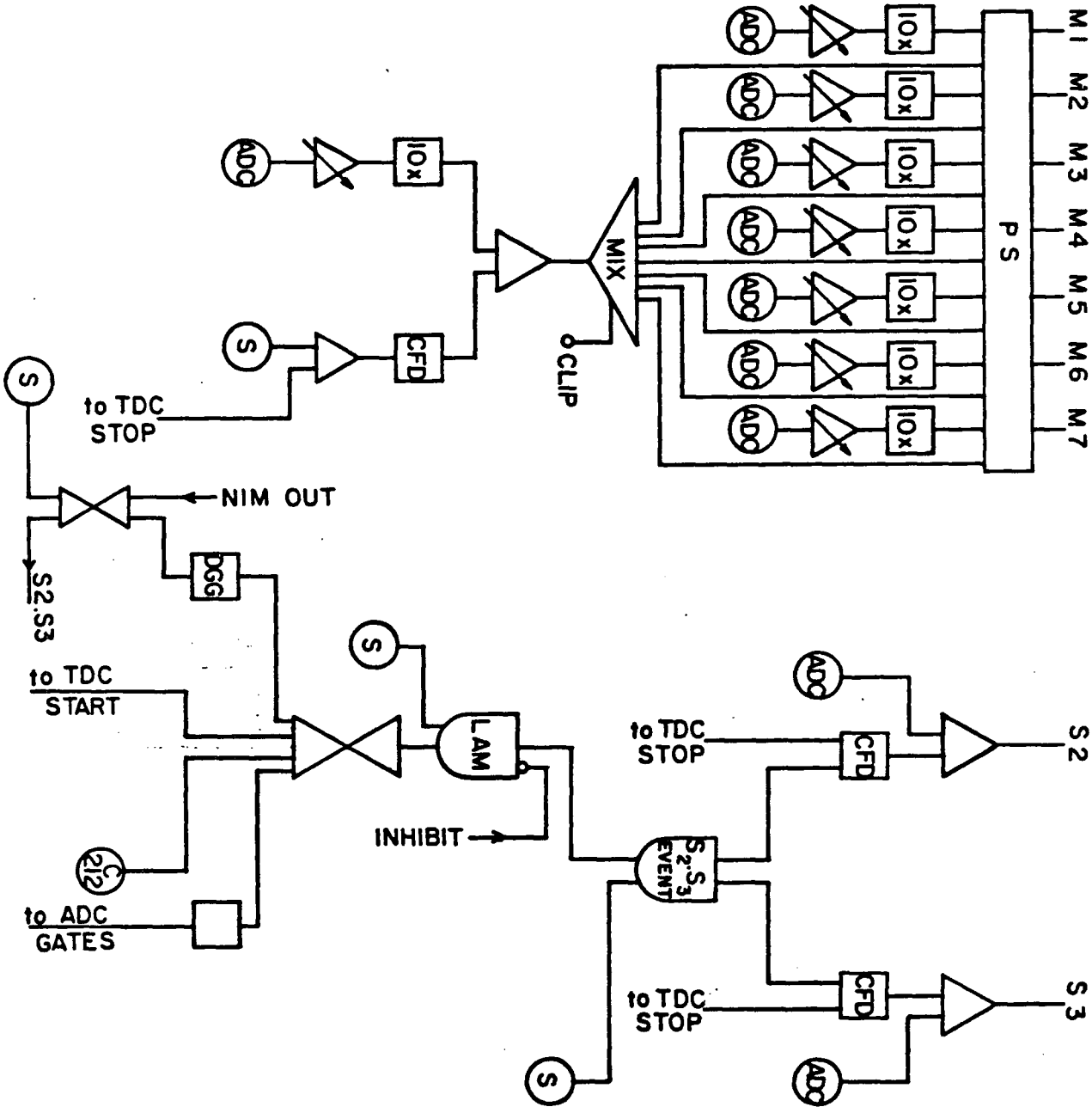

Fig. 2.6: Schematic of the electronics (1987 run)

CHAPTER 3

Data Analysis

The data analysis was performed using the VAX 8650 and VAX 780 computers at TRIUMF. The MULTI [48] written raw data were analyzed with MOLLI [49], the TRIUMF standard program for the off line manipulation of data, with user supplied subroutines. The different software cuts implemented to obtain the interaction loss for deuterons and protons will be discussed in this chapter.

3.1 Interaction loss of deuterons

The deuteron pulse height spectrum in MINA for all the events triggered is presented in Fig. 3.1 and shows the deuteron peak and a broad range of pulse heights from the events where the deuteron underwent a nuclear reaction, as well as from protons of varying energies which has scattered in the beamline. The primary means of identifying deuterons coming from the CH_2 production target was the time of the event trigger relative to the cyclotron R.F. Fig. 3.2 shows this time (for two 43 ns periods, for greater clarity) versus the energy deposited in the sodium iodide counter. The horizontal position is determined by relative flight time for each particle. The group marked 'a' are the deuterons produced in the CH_2 target, 'b' are the deuterons produced in the middle leg of the beamline near the beam-stop, and 'c' are the

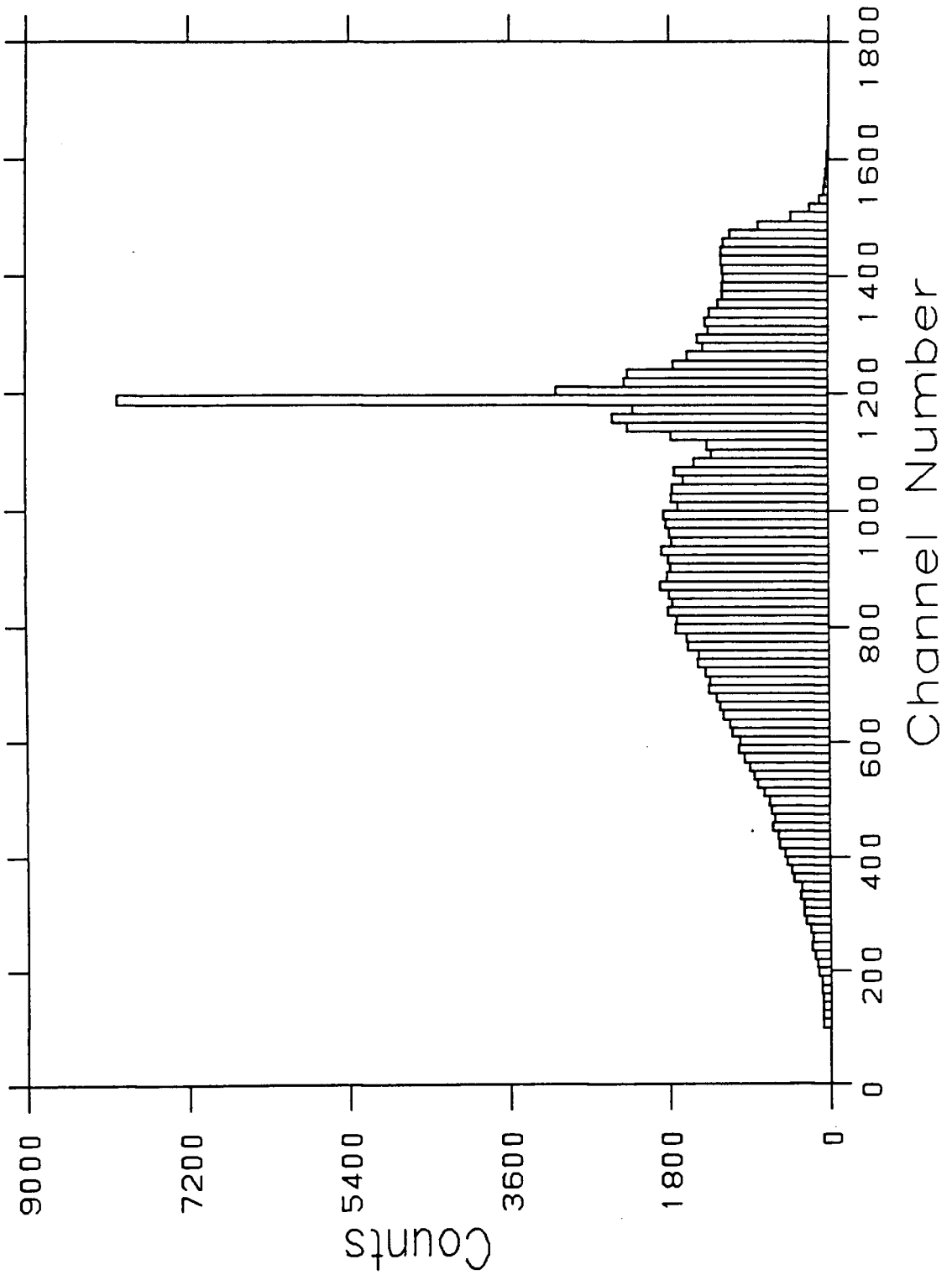

Fig. 3.1: A typical raw deuteron pulse height spectrum in MINA

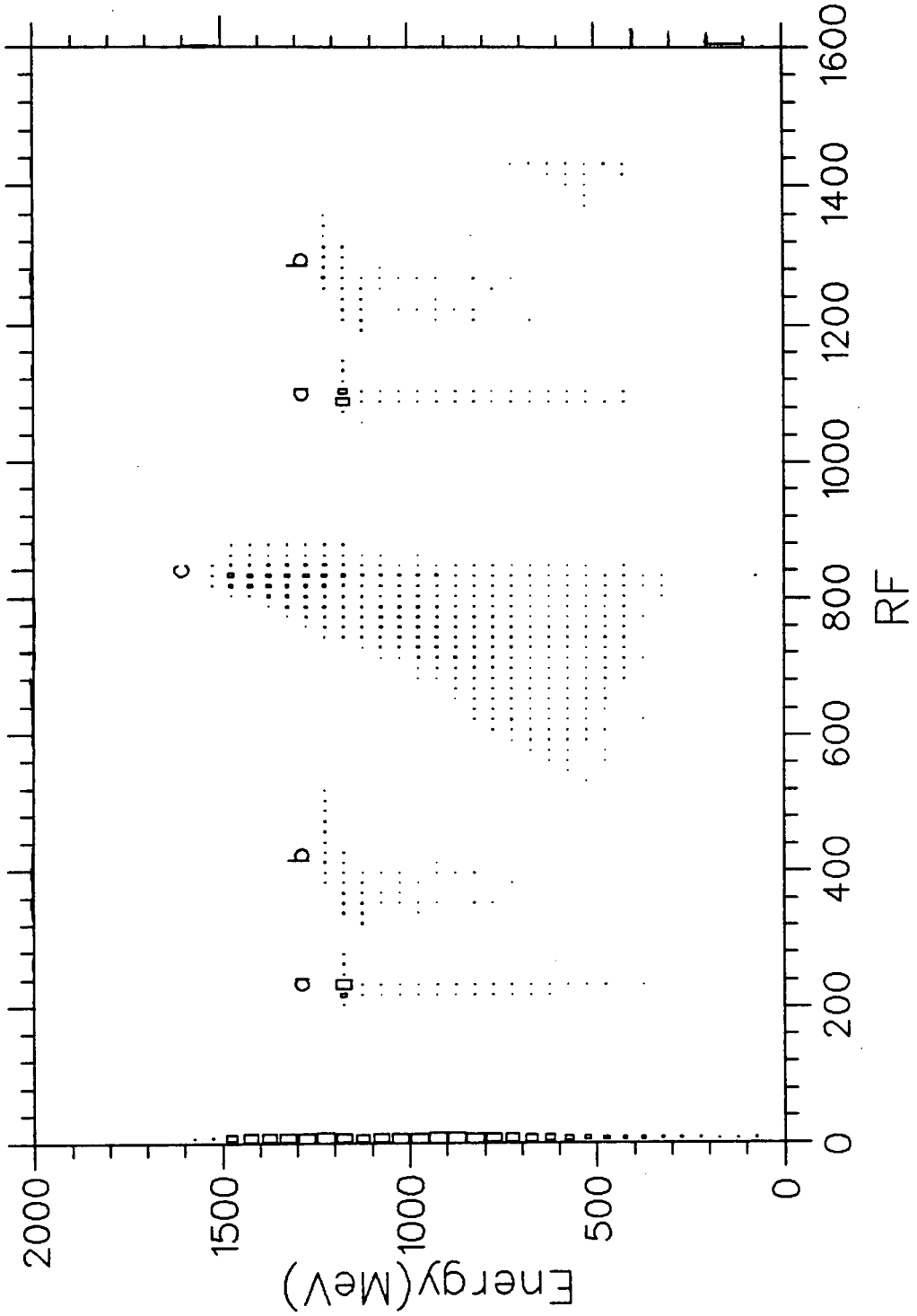

Fig. 3.2: **Two dimensional plot of energy deposited in MINA against RF time**

protons. The locus of the low-energy particles breaking off to the left of group 'c' matches that expected of 446 MeV protons which deflect into the vacuum vessel of the magnet B3, lose energy, and are scattered so as to emerge from B3 back on the beamline axis. The identification of deuterons and protons is confirmed by the time of flight between the plastic scintillators and by their pulse heights in the thick scintillator, but these parameters are not so sensitive. The multiwire proportional chambers were used to obtain position information of the deuterons. The X-Y position information from the wire chambers enabled us to confirm that the deuterons from the CH_2 target were being focussed as predicted by the beam transport calculations, that these deuterons did not strike the collimator, and that the range in angles was as calculated.

The events used in determining the NaI interaction loss had to satisfy the 'good deuteron' condition which consisted of tight restrictions or cuts on raw data which are as follows:

3.1.1 RF cut

The RF spectrum allows us to discriminate between deuterons of interest, other deuterons and protons. As mentioned earlier in this section the group marked 'a' are good deuterons (Fig. 3.2). A typical RF spectrum is shown in Fig. 3.3. The first pass at the data was to determine the RF cuts to be applied in the subsequent treatments to select only the good deuterons and thus eliminating useless data. The arrows indicate the cuts imposed on subsequent data.

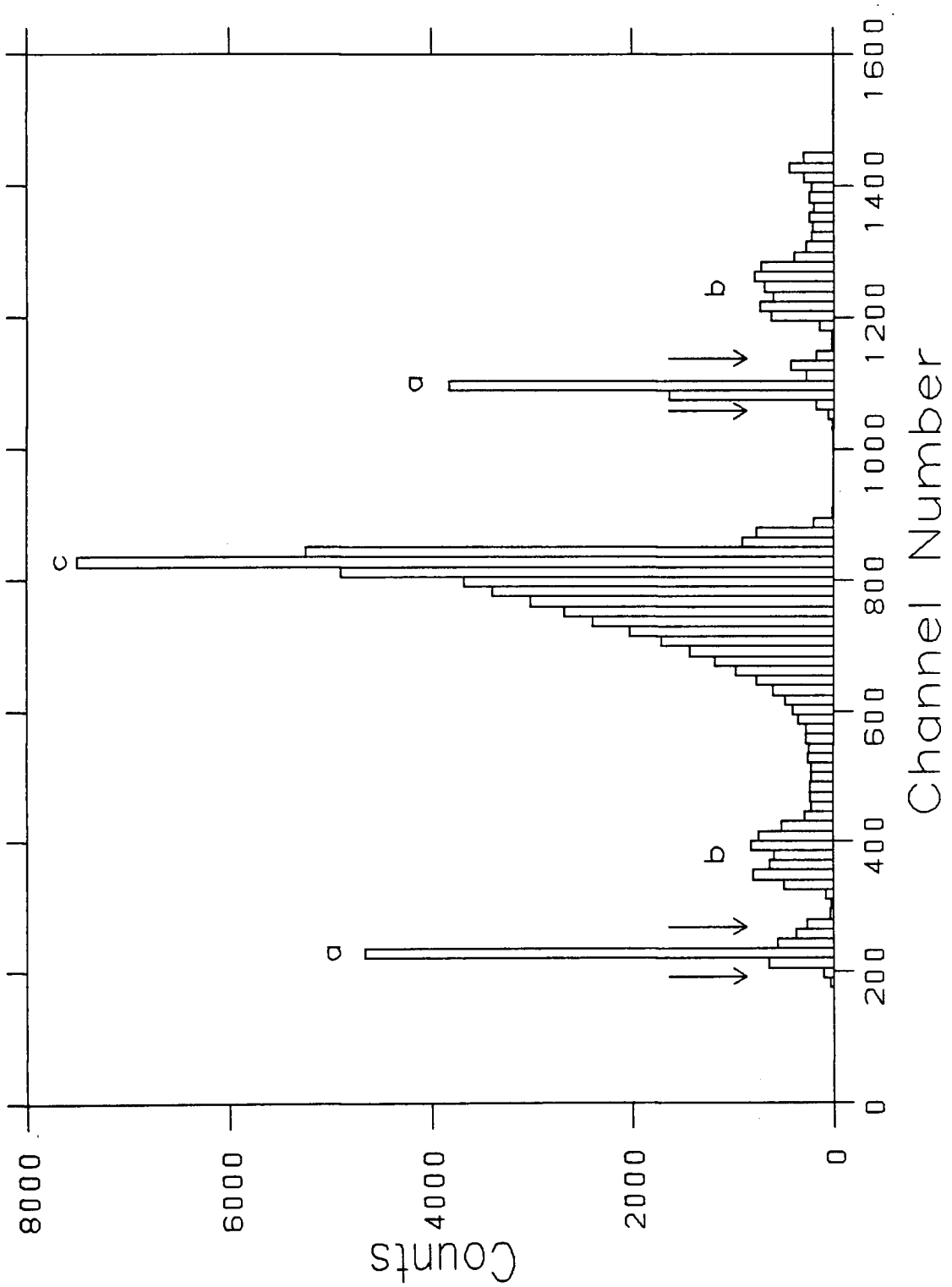

Fig. 3.3: A typical RF spectrum (deuteron run)

3.1.2 Time of flight cut

A typical raw spectrum of time of flight between two scintillators is shown in Fig. 3.4. Applying the RF cut for either deuterons or protons, one obtains a time of flight spectrum as shown in Fig. 3.5. This explains the origin of the two peaks in Fig. 3.4. The time of flight cut was selected using the information from Fig. 3.5.

3.1.3 Energy loss cut

The energy loss spectrum for the deuterons in the thick scintillator S_2 was generated from the raw data using RF and time of flight cuts (Fig 3.6). This spectrum was used to select the energy loss cut (dE/dx cut) and is also illustrated in the S_2 pulse height for protons.

3.1.4 Multiwire proportional chamber cut

Two wire chambers (MWPC1 and MWPC2) were used in the experiment. Each one has four outputs usually known as left, right, top and bottom outputs. Here we shall call the outputs of the first wire chamber L1, R1, T1, and B1 and for the second wire chamber as L2, R2, T2, and B2. TDC histograms for L1, R1, T1, B1, L2, R2, T2, and B2 were generated in the present experiment. A typical raw histogram for L1 is shown in Fig. 3.7. Four histograms X1, X2, Y1, and Y2 were then generated where

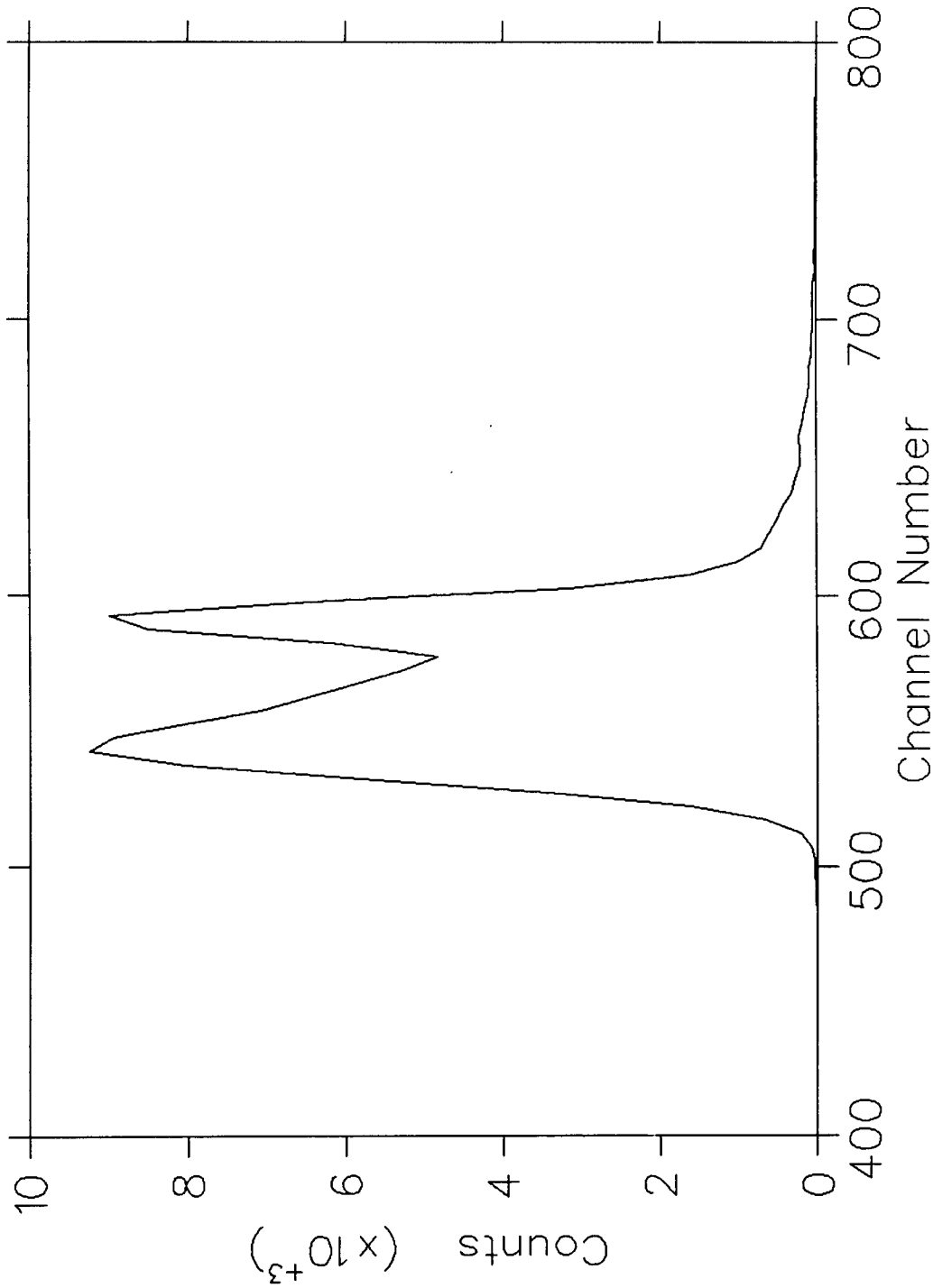

Fig. 3.4: **A typical raw spectrum of time of flight (TOF) between two scintillators**

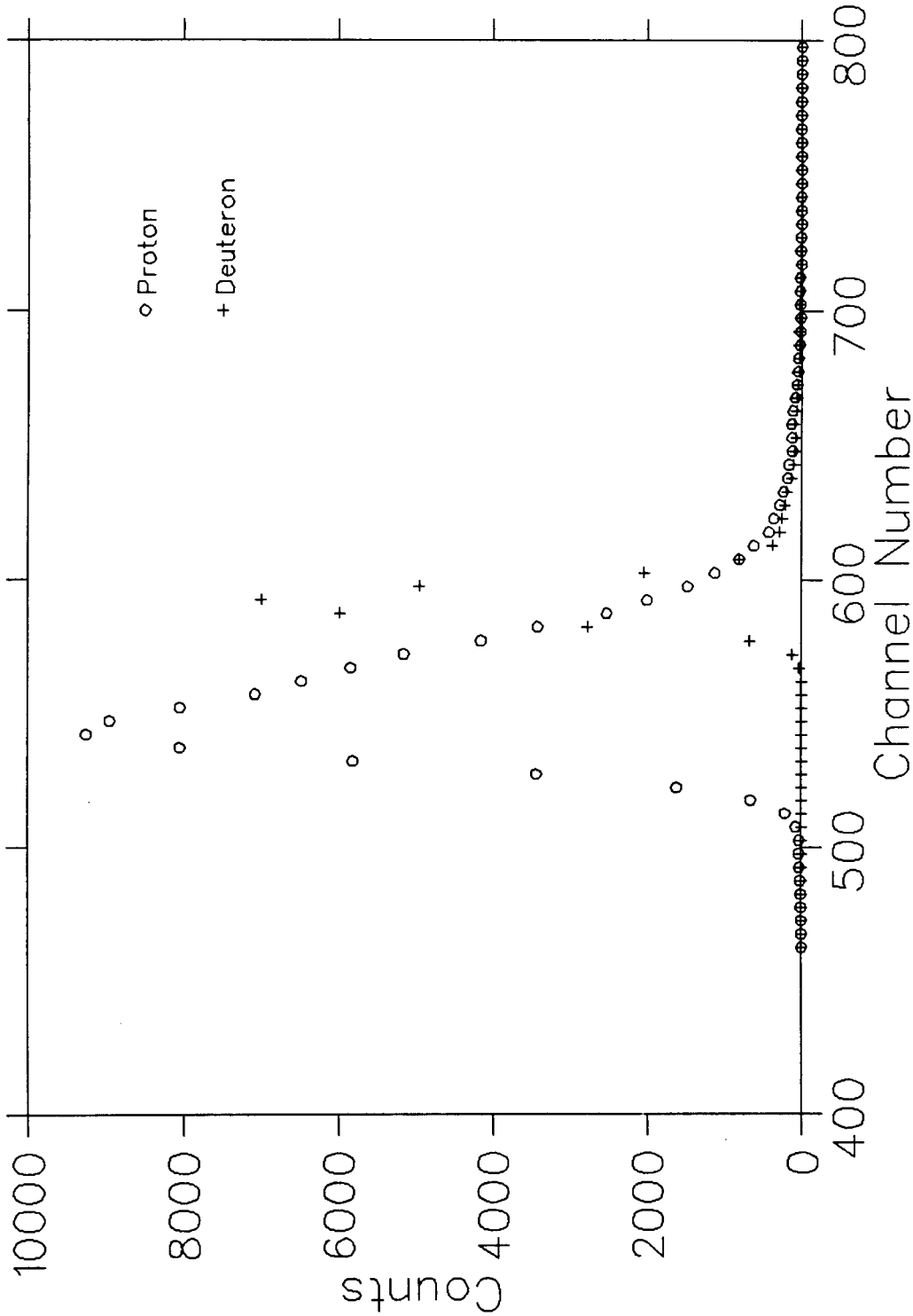

Fig. 3.5: A typical time of flight (TOF) spectrum with RF cut

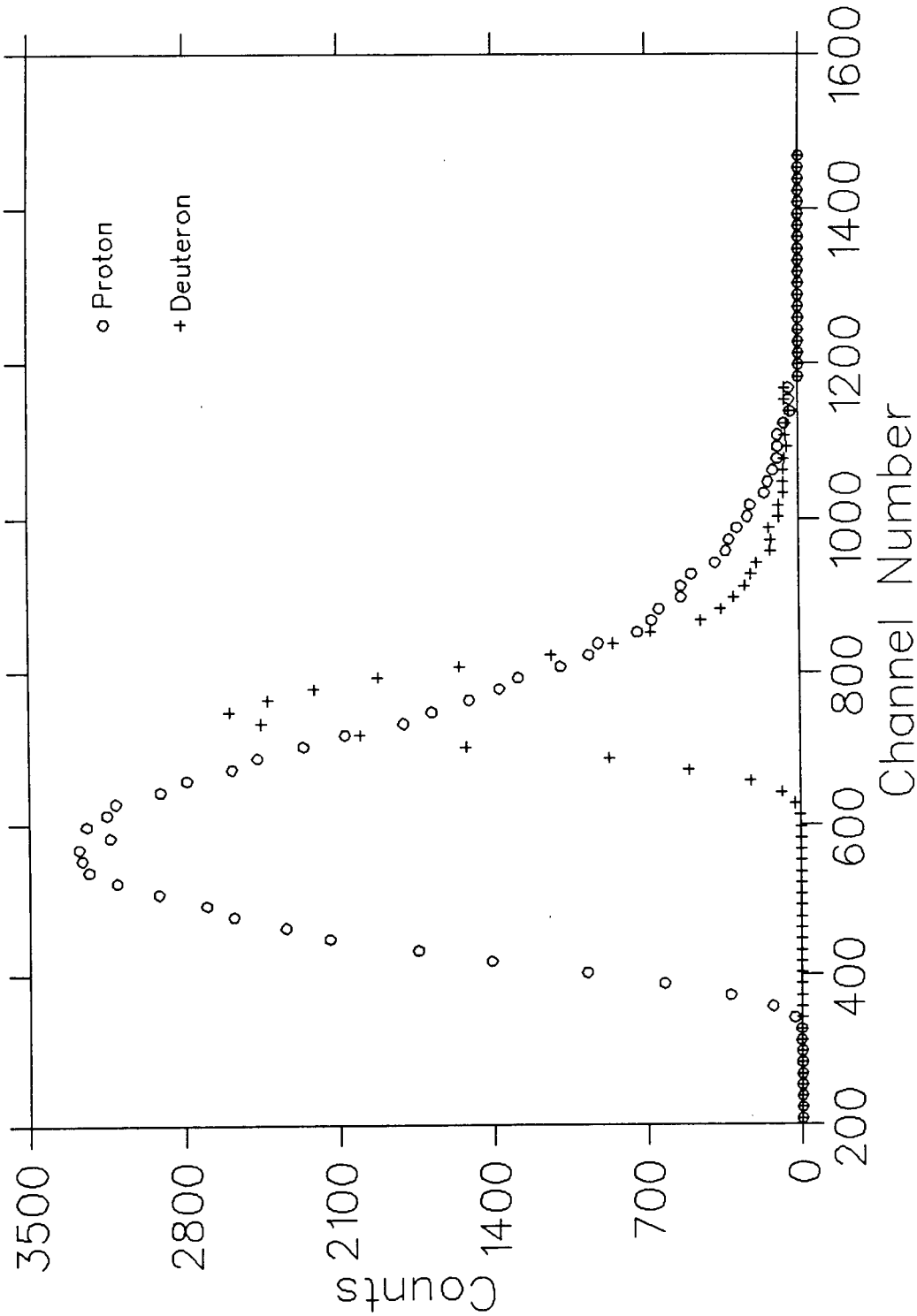

Fig. 3.6: **A typical deuteron energy loss spectrum in scintillator S2 with RF and TOF cuts**

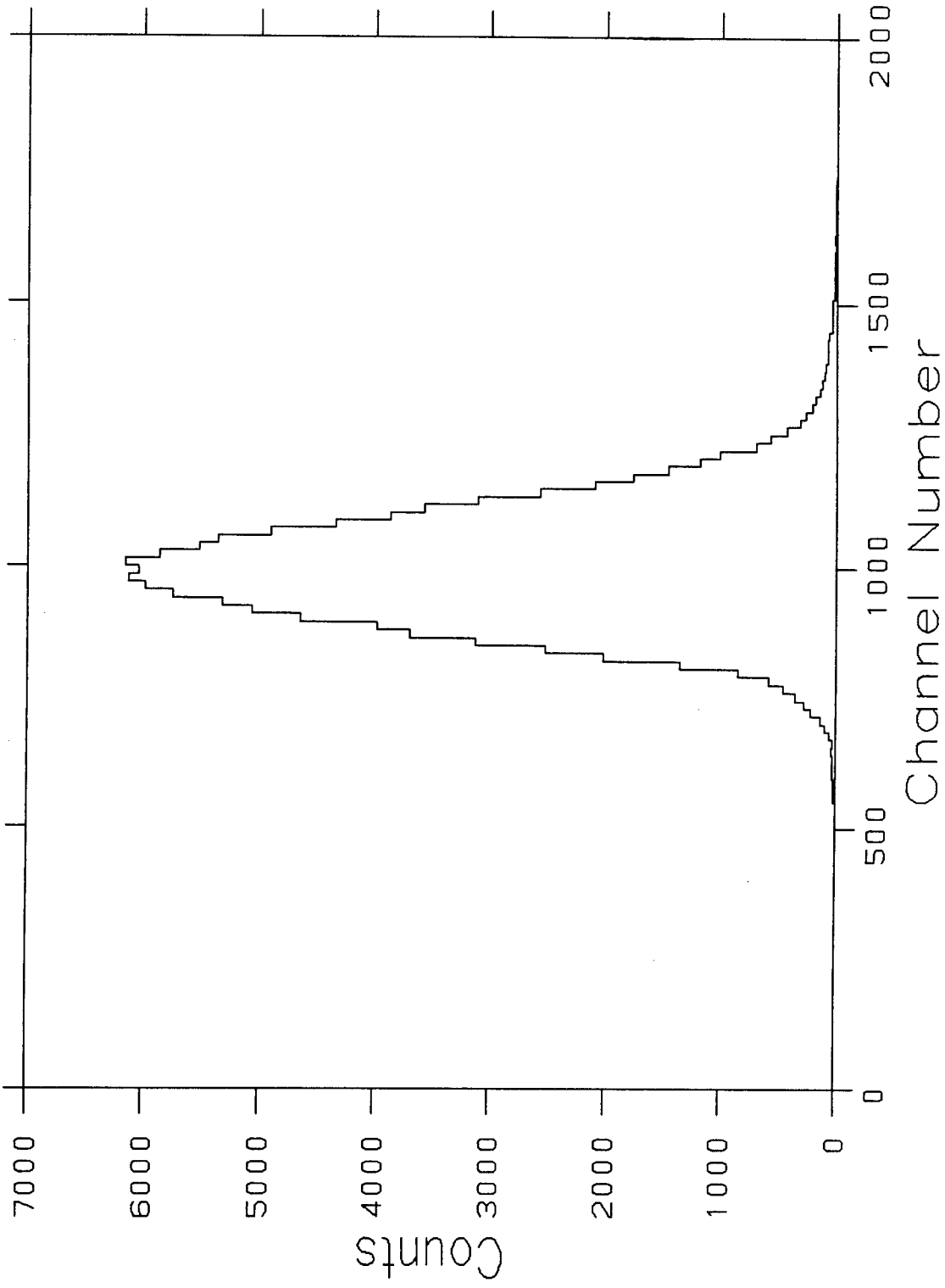

Fig. 3.7: A typical raw spectrum (L1) from a multiwire proportional chamber

$$X1 = L1 - R1; \quad X2 = L2 - R2$$

$$Y1 = B1 - T1; \quad Y2 - B2 - T2$$

These histograms show the deuteron beam profile in the X and Y directions in the two wire chambers. Two other histograms of the projected X, Y coordinates at the focal point X_{PRJ} = AX1 + BX2 and Y_{PRJ} = CY1 + DY2 were also generated where A = C = -3.2; B = D = 4.2.

A typical X1 and X_{PRJ} spectra with RF and time of flight cuts are shown in Figs. 3.8 and 3.9 respectively. The wire chamber cuts were selected from the X1, X2, Y1, Y2, X_{PRJ} and Y_{PRJ} spectra.

After implementing RF, time of flight, energy loss (dE/dX) and wire chamber cuts, any particles other than deuterons and any deuterons other than those produced in the CH_2 target were removed. Using all these cuts the deuteron energy spectrum in MINA was generated and was used in determining the sodium iodide response. A typical deuteron energy spectrum in MINA is given in Fig. 3.10. The resolution of MINA is very good for these deuterons - no worse than 0.7% FWHM in the peak as shown in Fig. 3.11.

3.1.5 Energy calibration

The protons with 446 MeV energy from the cyclotron produced deuterons of 291.6 MeV energy through the reaction $p+p \rightarrow d+\pi^+$.

The energy lost by the deuterons traversing the distance between the exit window and MINA was calculated. Considering the stainless steel exit window, plastic scintillators and the aluminum layer in the front

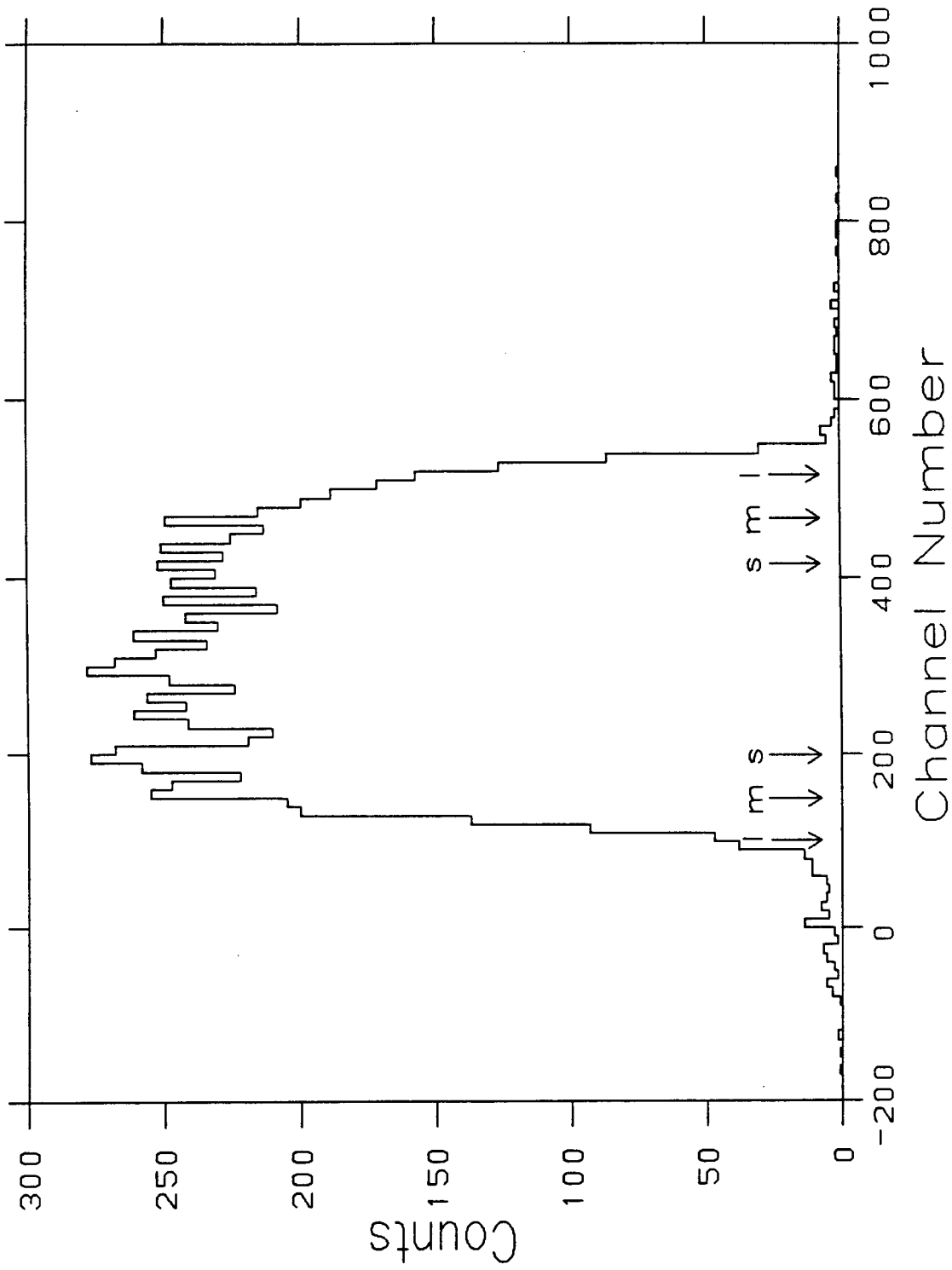

Fig. 3.8: A typical spectrum (X1=L1-R1) from a multiwire proportional chamber with RF and TOF cuts

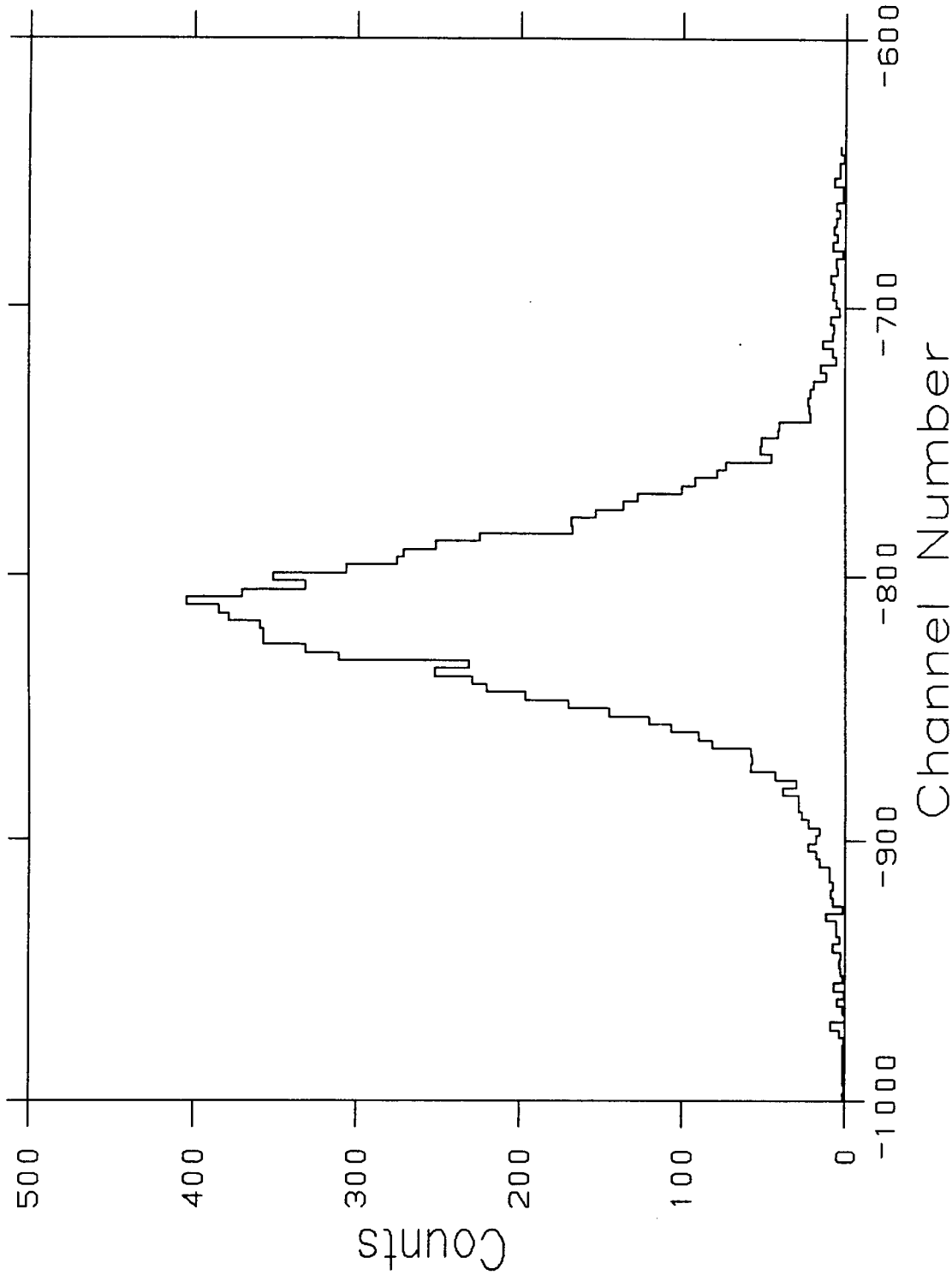

Fig. 3.9: A typical spectrum (X_{PRJ} = AX1+BX2) with RF and TOF cuts

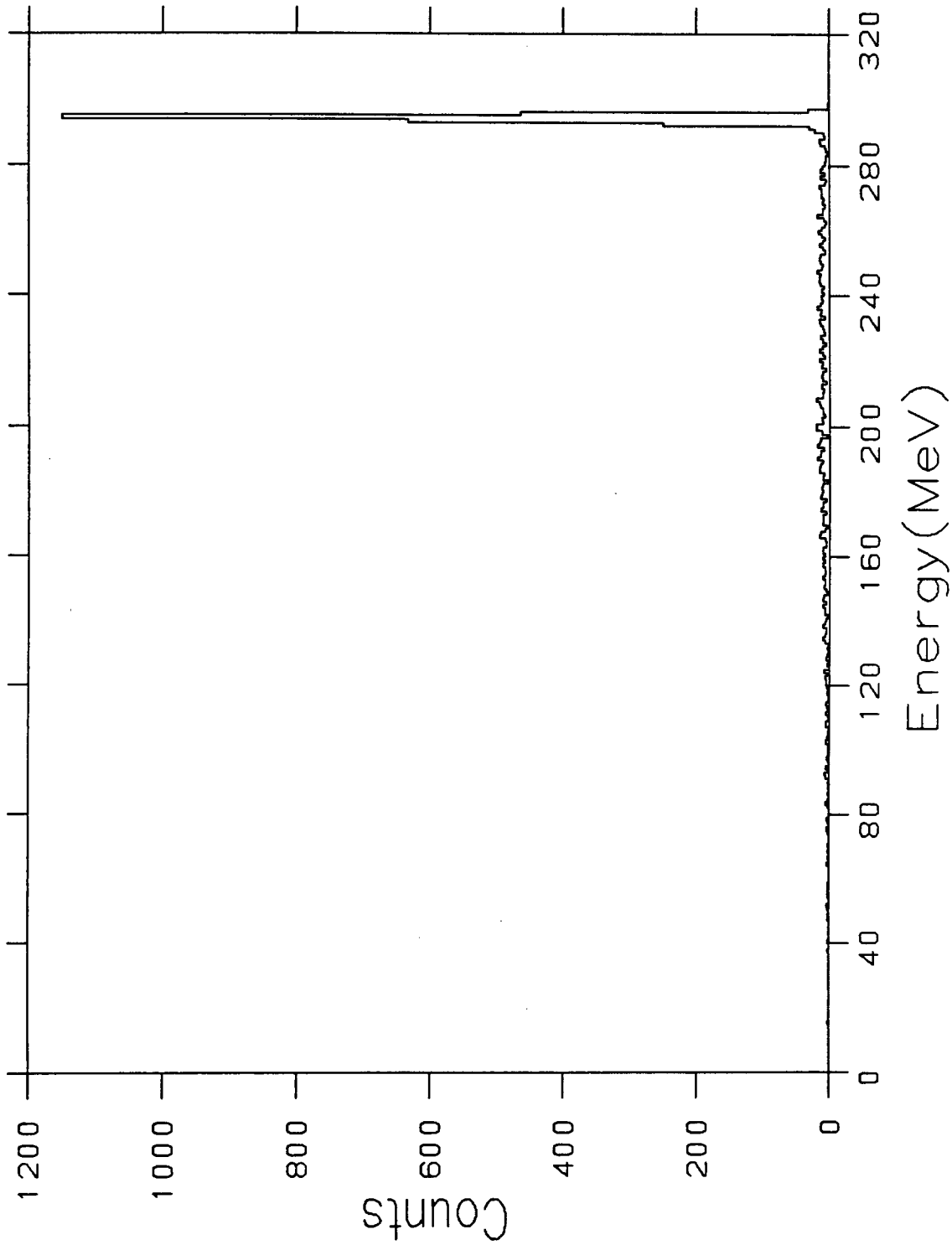

Fig. 3.10: A typical deuteron energy spectrum in MINA

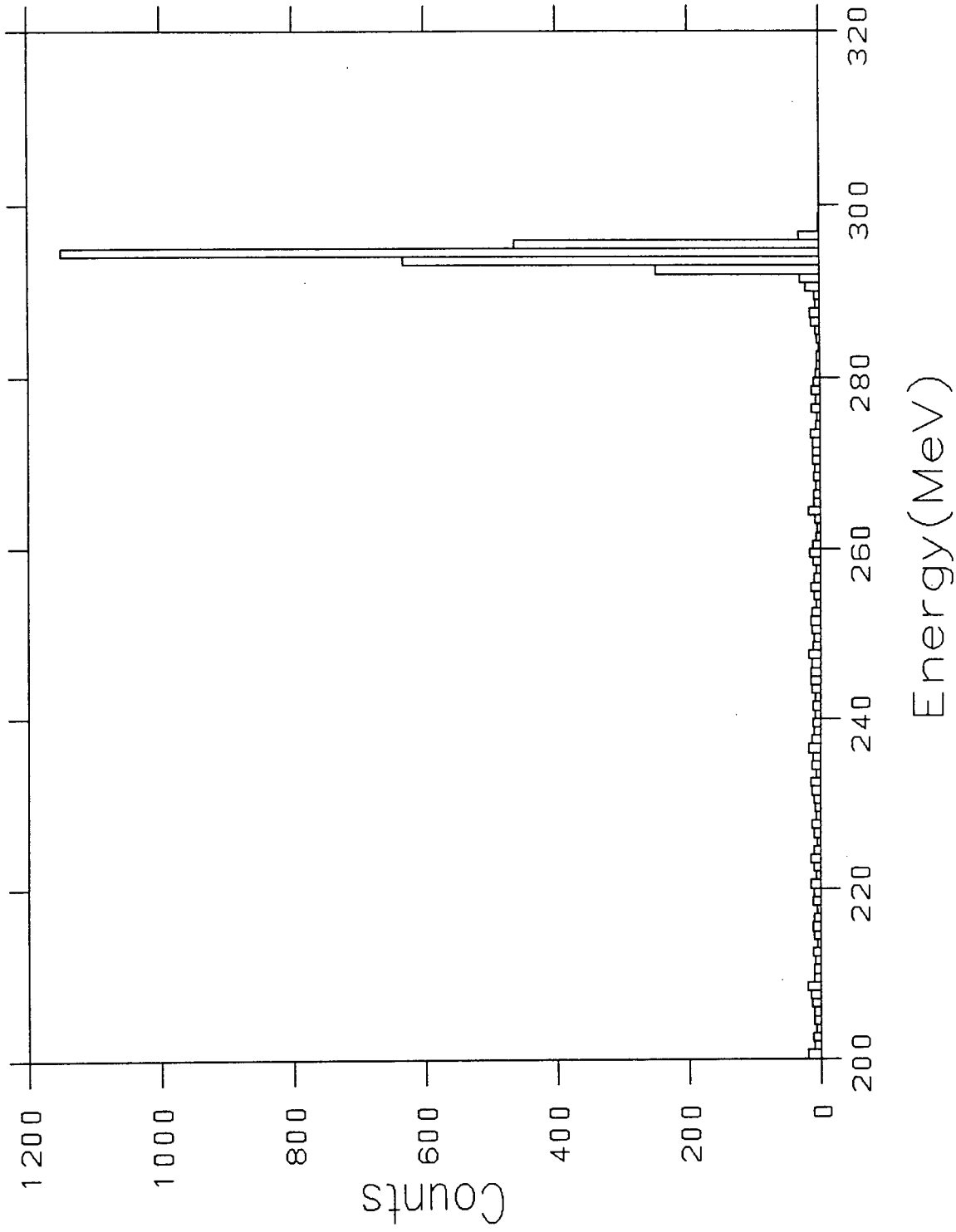

Fig. 3.11: A typical deuteron energy spectrum showing MINA resolution

face of MINA, the deuterons lost about 14.8 MeV. The 276.8 MeV energy deuteron peak was obtained at channel number 1190 while the MINA pedestal was obtained at channel number 94. Using these 2 points the MINA energy was calibrated.

3.2 Interaction loss of protons

The analysis of the data for the interaction loss for protons will now be discussed. The September '86 run, used scattered protons from the p+p→p+p reaction and will be discussed in section 3.2.1. The March '86 run used the direct proton beam into the NaI, and will be discussed in section 3.2.2.

3.2.1 Protons from p+p→p+p in NaI detectors

During the September '86 run, protons of different energies were used while TINA and MINA were placed at different angles with respect to the incoming beam. The two crystals were used in coincidence. The energies of the incoming proton beam and the corresponding energies of the protons at TINA and MINA have already been given in Table 2.2 (p. 19).

The RF spectrum for TINA and MINA (RFT and RFM as described in section 2.5) were generated. A typical RFT spectrum is shown in Fig. 3.12, which shows two proton peaks separated by 43 ns. RF cuts for TINA

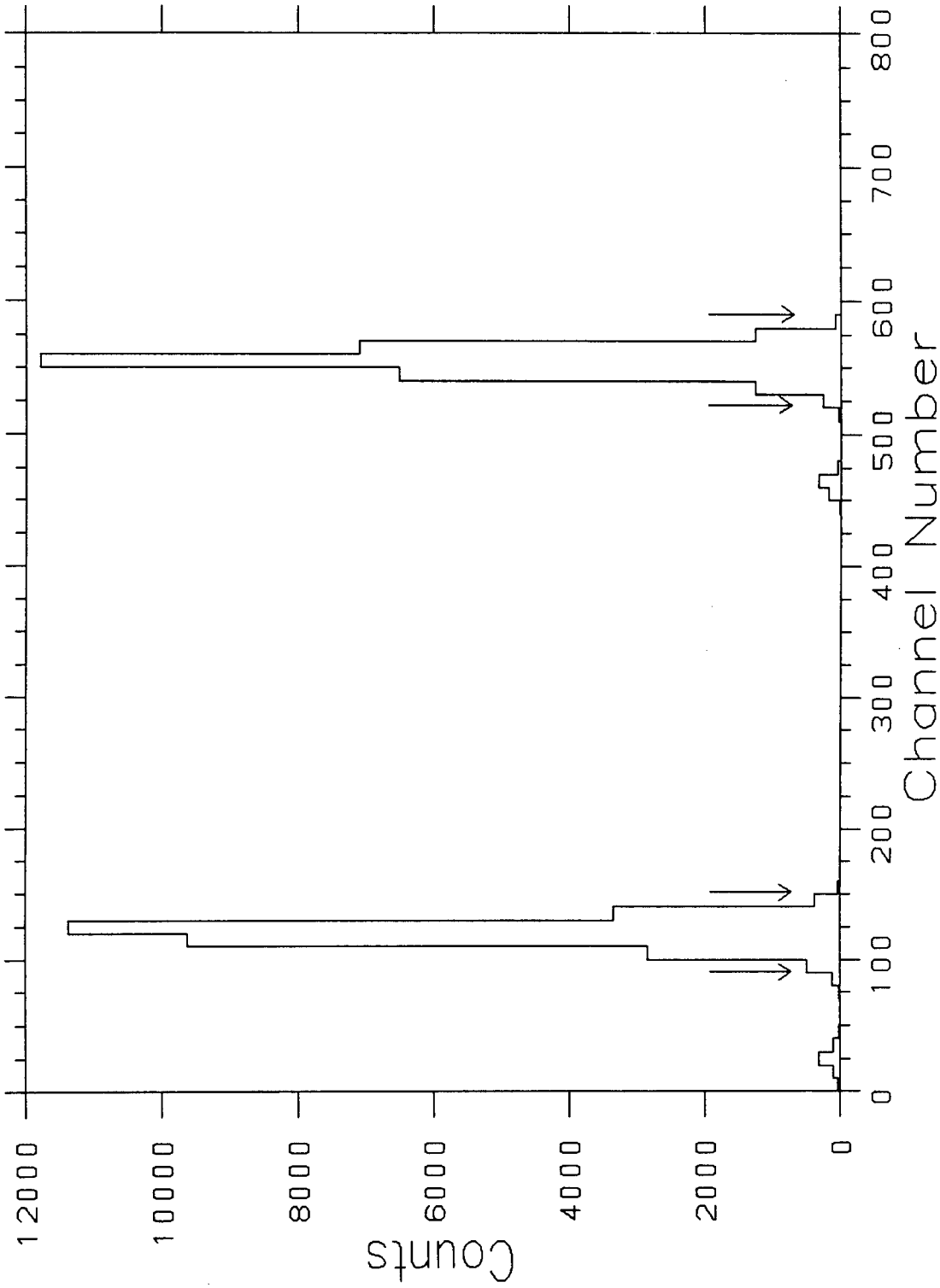

Fig. 3.12: A typical RF spectrum (proton run)

were chosen from this spectrum as shown by the arrows. Similarly RF cuts for MINA were also chosen from a RFM spectrum.

A scatter plot of TINA energy versus MINA energy was generated (Fig. 3.13) which shows the range of proton energies in TINA and MINA. In the subsequent analysis while generating energy spectra in TINA, a restriction on the MINA energy spectrum was imposed and vice versa. These cuts were selected from the scatter plot which make sure that while a scattered proton of full energy is detected in one of the detectors, the recoil proton is detected in the other. The final proton energy spectra in TINA and in MINA were obtained using the RF and the scatter plot cuts.

Similar techniques were applied to generate the energy spectrum in TINA and in MINA for empty target runs. After normalization, the empty target spectrum was subtracted from the corresponding full target proton energy spectrum to obtain the background subtracted final proton energy spectrum; a typical one is shown in Fig. 3.14.

When the outgoing protons leave the target vessel on their way towards the detector, they lose some energy traversing half of the distance of the target vessel, plastic scintillators and the Al layer present in the front face of TINA and MINA. The actual energies at the crystals were given in Table 2.2 (p. 19).

TINA and MINA energies were then calibrated using data from different runs. The TINA energy calibration curve is shown in Fig. 3.15.

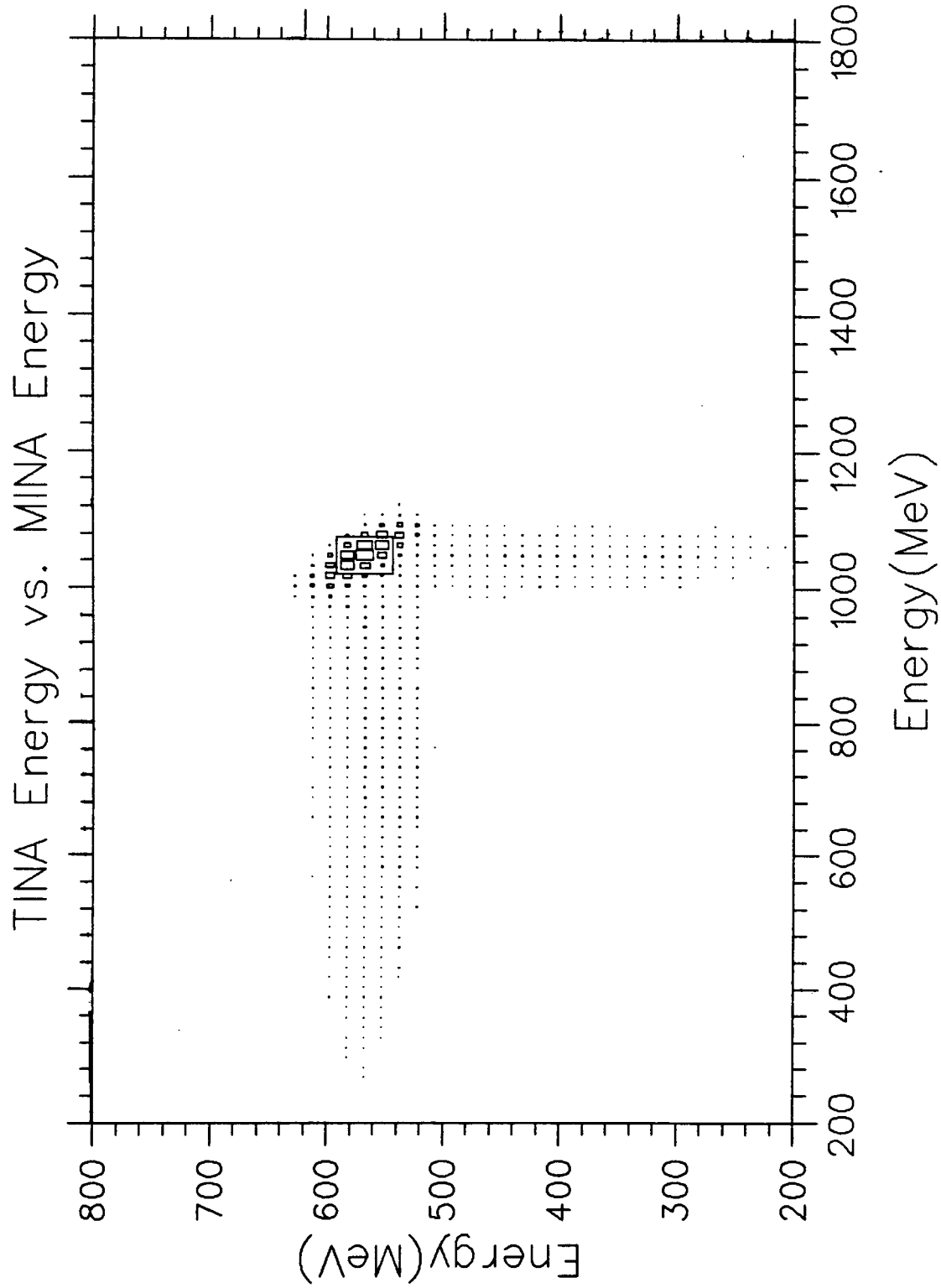

Fig. 3.13: Two dimensional plot of energy deposited in TINA against energy deposited in MINA

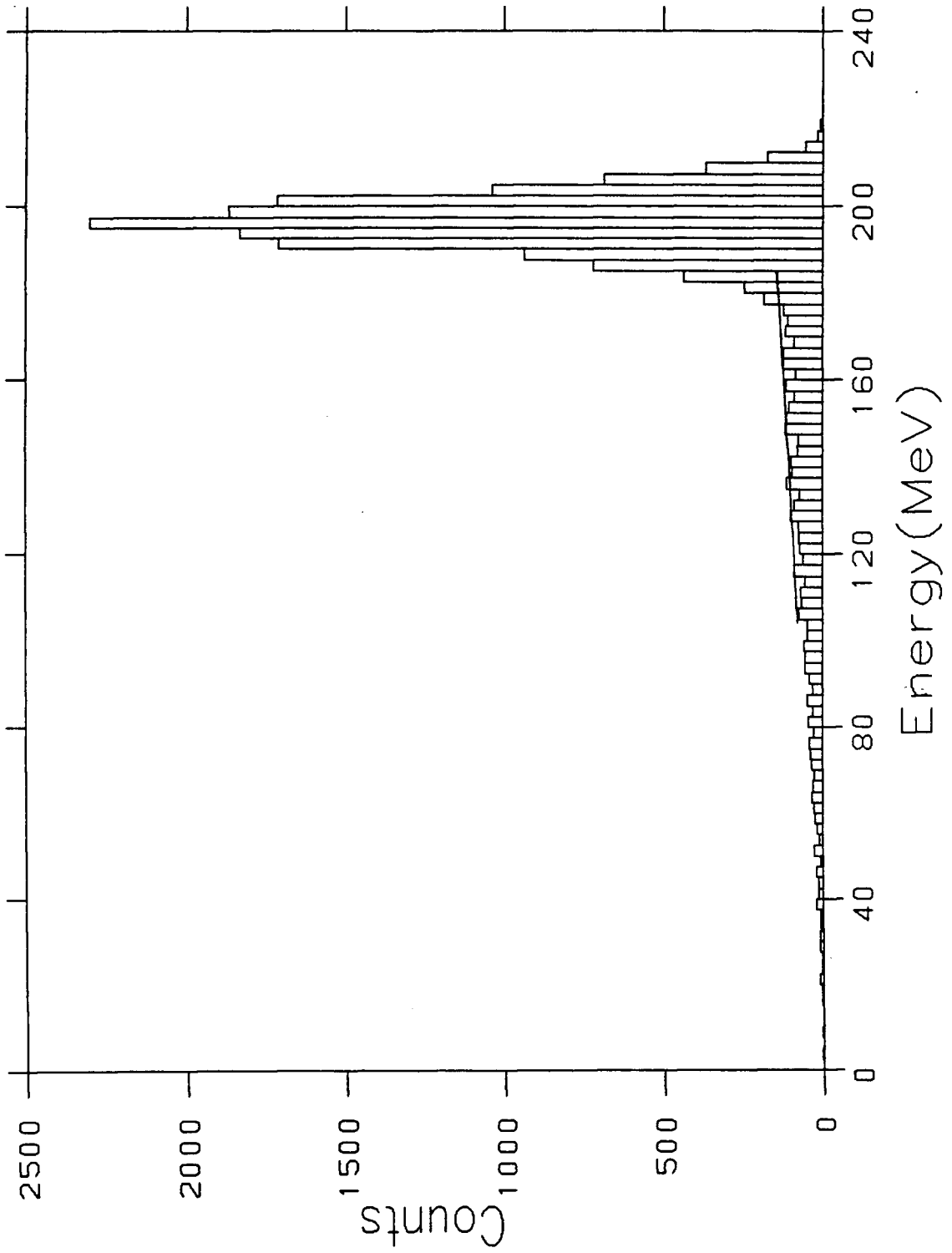

Fig. 3.14: A typical background subtracted proton energy spectrum

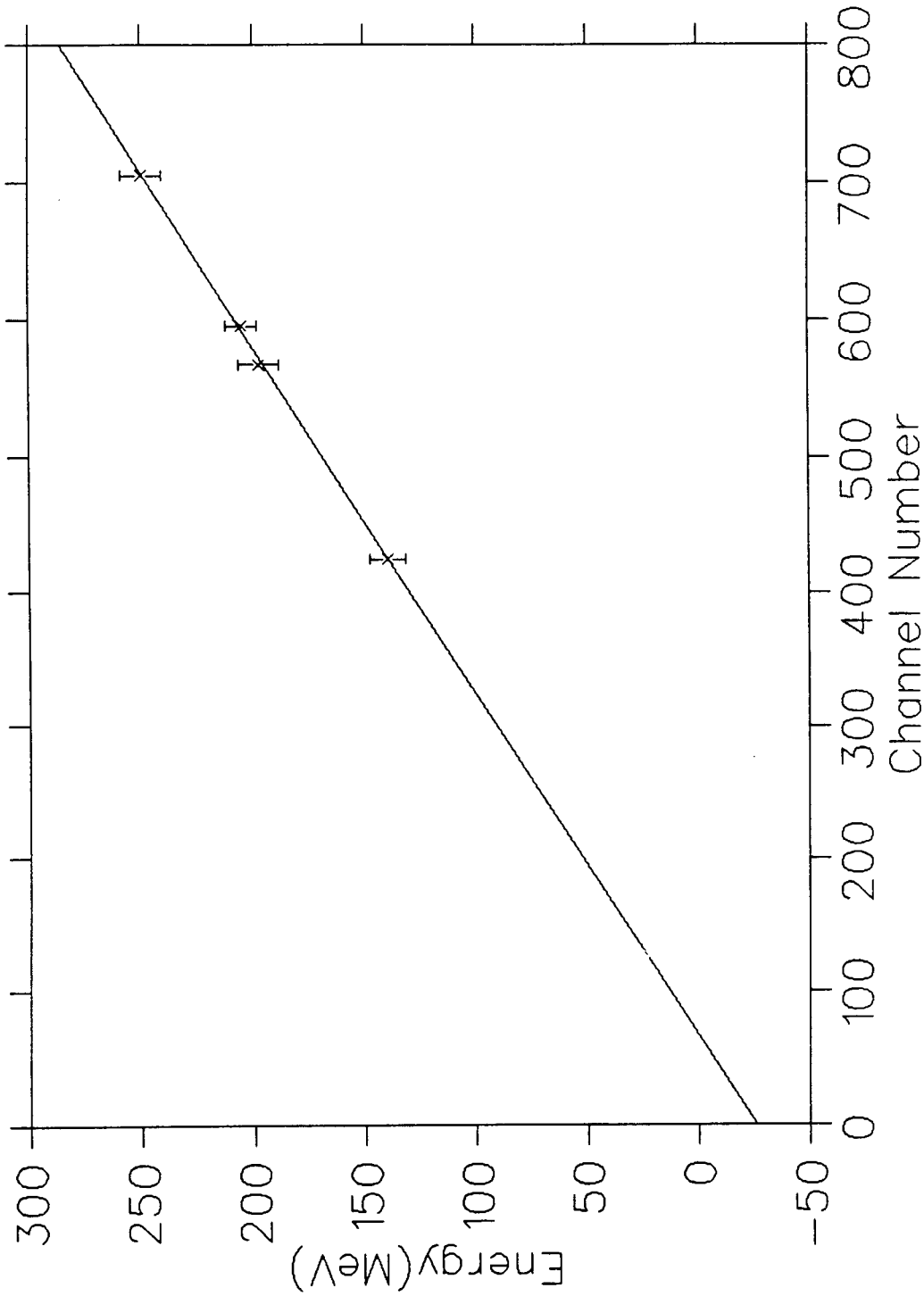

Fig. 3.15: Energy calibration of TINA

3.2.2 Direct proton beam in a NaI detector

In the March '87 run, a direct proton beam of 348 MeV and 446 MeV was used with TINA as the detector. As usual the RF cut was selected from the RFT histogram.

The proton energy spectrum in the thick scintillator (ES2) was then obtained using an RF cut. The dE/dX cut was selected from this spectrum. The time of flight spectrum was also generated with an RF cut. The cut for the time of flight of the protons between two scintillators was then selected. For the direct beam the vast majority of events pass all these cuts.

Using RF, dE/dX and the time of flight cuts the final proton energy spectrum was obtained. A typical proton energy spectrum is shown in Fig. 3.16.

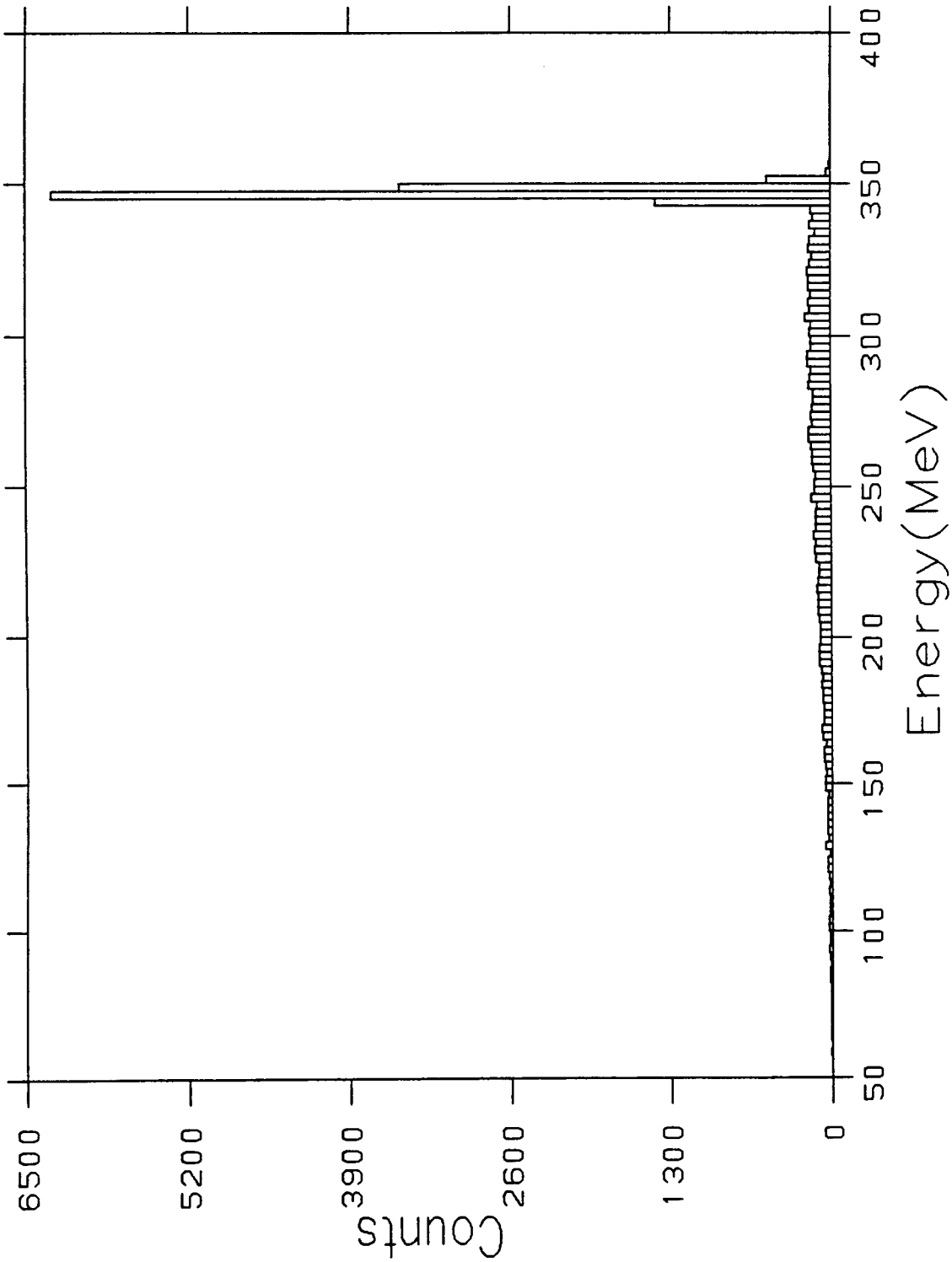

Fig. 3.16: A typical proton energy spectrum in TINA

CHAPTER 4

Results and Discussion

4.1 Deuteron interactions

In the deuteron energy spectrum in MINA (Fig. 3.10) the tail was separated from the peak by a cut in the spectrum at 5 MeV below the maximum of the peak. We also consider this cut-off at 10 MeV below the peak to separate the non interacting peak from the interaction tail. With each cut imposed, the peak to total counts ratio improved slightly. Table 4.1 shows a comparison of tail to total counts ratio or interaction loss with different cuts both at 5 and 10 MeV below the peak cut-off point.

The final tail to total counts ratio or interaction loss for the 276.8 MeV deuterons in the sodium iodide crystal was found to be 39.5 ± 1.7% and 38.4 ± 1.7% for cut off at 5 MeV and 10 MeV below the peak, respectively, where the errors given are purely statistical. The value for the interaction loss is relatively insensitive to quite severe cuts on RF, time of flight, and energy loss. This value for the interaction loss is similar to that found for germanium detectors, viz. ~40% [29].

Using standard RF, TOF and dE/dX cuts, we have also studied the sensitivity of the interaction loss to X, Y cuts from wire chamber 1. Loose, medium and severe cuts were imposed on the X spectrum which are shown by arrows marked ℓ, m, and s respectively in Fig. 3.8 (p. 39).

Table 4.1

Interaction loss of deuterons using different cuts

Cut	Cut off at 5 MeV below the peak	Cut off at 10 MeV below the peak
	$\frac{\text{Tail}}{\text{Total}}$* %	$\frac{\text{Tail}}{\text{Total}}$* %
RF	41.7 ± 1.1	40.0 ± 1.1
RF and time of flight	42.3 ± 1.1	39.6 ± 1.0
RF, time of flight and dE/dX	40.9 ± 1.1	39.2 ± 1.0
RF, time of flight, dE/dX and wire chamber	39.5 ± 1.5	38.4 ± 1.5

* Error quoted is only statistical

Similar cuts were imposed on the Y spectrum and it was found that the interaction loss is more or less insensitive to these cuts as shown in Table 4.2.

Table 4.2

Effect of different X, Y cuts on the interaction loss of deuterons

Cut		Cut off at 5 MeV below the peak	Cut off at 10 MeV below the peak
		$\frac{\text{Tail}}{\text{Total}}$ * %	$\frac{\text{Tail}}{\text{Total}}$ * %
X Loose	Y Loose	40.6 ± 1.1	39.1 ± 1.1
	Y Medium	40.7 ± 1.1	39.1 ± 1.1
	Y Severe	40.6 ± 1.4	38.9 ± 1.3
X Medium	Y Loose	40.6 ± 1.2	38.9 ± 1.1
	Y Medium	40.7 ± 1.2	39.0 ± 1.2
	Y Severe	40.8 ± 1.5	38.8 ± 1.4
X Severe	Y Loose	41.0 ± 1.4	39.4 ± 1.4
	Y Medium	41.0 ± 1.4	39.4 ± 1.4
	Y Severe	41.1 ± 1.8	39.1 ± 1.7

* Error quoted is only statistical

4.2 Proton interactions

In the proton energy spectrum (Fig. 3.14) the interaction tail was separated from the peak by a cut in the spectrum at 10 MeV below the maximum of the peak. If we look at the spectrum carefully we see that past the 10 MeV cut, a few bins contain counts some portion of which could be attributed to the tail and some to the peak. A line was drawn in the tail region (as shown in Fig. 3.14) which was extended up to the

cut off line, 10 MeV below the peak. Counts above this line in these bins were attributed to the peak and the rest to the tail.

Thus the tail to total (tail + peak) ratio or the interaction loss was calculated. This ratio was also calculated in the same way with the cut 5 MeV below the peak. Similarly in the final proton energy spectra of the March '87 run (Fig. 3.16), the 10 MeV and 5 MeV cut off points were used to calculate the tail over total ratio. The results from both the runs are given in Table 4.3.

4.3 Discussion

4.3.1 Proton data

In both the March '86 and the September '87 runs, the thickness of all the materials present in the beam path towards the detector was calculated in g/cm^2. Considering the interaction loss in each of these materials (hydrogen, plastic, aluminum layer in front face of the detector etc.) to be 1% per g/cm^2 [47], the total interaction loss was then calculated. The interaction loss in these materials introduces a correction and one of the systematic uncertainty in our final results of the proton and the deuteron interaction loss in NaI was taken to be 20% of this correction. The ambiguity of separating the reactions into elastic and inelastic regions also introduces an uncertainty in the tail to total ratio. The effect of changing the position of the cut by 5 MeV on the present data is on the average ~1.5%. We have considered half of

Table 4.3

Results of the interaction loss of protons with 5 and 10 MeV cuts

Proton energy (in MeV)	Interaction Loss (%)* Cut off at 10 MeV below peak	Cut off at 5 MeV below peak
139.3	13.1 ± 0.4	14.2 ± 0.4
184.7	21.0 ± 0.2	22.9 ± 0.2
196.9	21.7 ± 0.5	23.1 ± 0.5
204.7	21.7 ± 0.2	22.9 ± 0.2
210.6	24.2 ± 0.2	25.3 ± 0.2
227.7	27.5 ± 0.2	29.0 ± 0.2
235.8	29.5 ± 0.4	31.0 ± 0.4
249.3	29.1 ± 0.4	30.7 ± 0.4
288.2	38.4 ± 0.6	40.2 ± 0.6
344.9	45.5 ± 0.7	47.2 ± 0.7
345.7**	45.8 ± 0.8	47.2 ± 0.8
443.9**	58.4 ± 0.4	59.9 ± 0.4

* Error quoted is only statistical

** From the March '87 run

this difference as the uncertainty. Hence the error quoted in our final results (Table 4.4) includes the statistical error as well as the systematic errors. The statistical error and the systematic errors were added in quadrature to obtain the final error.

Table 4.4

Present results for the proton interaction loss in NaI detectors using a cut 10 MeV below the peak

Energy (MeV)	Interaction loss* (%)
139.3	13.1 ± 0.9
184.7	21.0 ± 0.9
196.9	21.7 ± 1.0
204.7	21.7 ± 0.9
210.6	24.2 ± 0.9
227.7	27.5 ± 0.9
235.8	29.5 ± 1.0
249.3	29.1 ± 0.9
288.2	38.4 ± 1.1
344.9	45.5 ± 1.1
345.7	45.8 ± 1.2
443.9	58.4 ± 0.9

* Total error incorporating statistical and systematic

In the present experiment, the interaction loss of protons in NaI obtained over the range 139-444 MeV and tabulated in Table 4.4 is somewhat smaller than the calculated values [1,26]. The calculated values of Goulding and Rogers are slightly higher than the values of Measday and C. Richard-Serre. Goulding and Roger's experimentally measured loss at 146 MeV is also larger than our measured value. Because of these inconsistencies we have decided to recalculate the interaction loss. The procedure we have undertaken is as follows:

The tabulated values of energy E and dE/dX for proton in NaI obtained from the CERN report [1] were fitted, using TRIUMF MINUIT program, with a function

$$Y = Ax^{-B} + C \qquad (4.1)$$

where Y is the fitted dE/dX, X is the energy. About 1% uncertainty was assigned to the dE/dX data up to 300 MeV and 0.5% up to 500 MeV. Parameters obtained from the best fit are A = 213.8940, B = 0.8976 and C = 0.8949.

The original dE/dX data and the data obtained using the best fit parameters are shown in Table 4.5 for comparison.

To calculate the interaction loss, for convenience it was assumed that the NaI crystal was divided into cells of various thickness where, in each cell, protons lose 1 MeV in energy. We started our calculation assuming 500 MeV incoming protons and continued dividing the crystal into cells until the proton energy dropped to 150 MeV. Thus there were 350 cells of various thickness. We were particularly interested in the

Table 4.5

Comparison of dE/dX values

Energy (MeV)	dE/dX (MeV/g/cm^2) from CERN report	dE/dX (MeV/g/cm^2) from fit
100	4.330	4.322
200	2.734	2.734
300	2.167	2.173
400	1.881	1.882
500	1.711	1.703

energy range of 150-500 MeV because there is a lack of data in this energy range.

The total fraction of interaction is given by $f=1-\exp(-\sum_i n_i\sigma_i)$ where n_i is the number of atoms/cm^2 in the ith cell and σ_i is the reaction cross section in that cell. For each of the 1 MeV cells, the range of protons is g/cm^2 was calculated using the fitted dE/dX value for the proton energy in that cell. Using the range values for the 1 MeV cells, the number of atoms/cm^2 (n_i's) were then calculated. Knowing n_i's and σ_i's for each cell, the interaction loss for protons in the energy range

151-500 MeV can be calculated. We started with 151 MeV protons whose interaction loss could be found using the following expression:

$$I_{151} = n_{151}\sigma_{151} + I_{150}\,(1 - n_{151}\sigma_{151}) \qquad (4.2)$$

where I_{150} is the interaction loss of 150 MeV protons in NaI, the value of which was obtained from the CERN report [1]. Thus the interaction loss for 152 MeV proton, I_{152} was computed using the value obtained for I_{151} and so on.

We first assumed an energy independent cross section σ in the energy range 151-500 MeV and the interaction loss of proton were calculated. The calculated values were then compared with our measured values using χ^2 minimization technique keeping σ as a free parameter. From the best fit, σ = 1273 ± 24 mb was obtained.

Since the reaction cross section σ is not actually energy independent, we tried to calculate the loss assuming an energy dependent σ. We have fitted the existing results of reaction cross-sections versus energies [1,16] with an energy dependent function

$$\sigma = p + QE + RE^2 \qquad (4.3)$$

and obtained the parameters p = 1634.27, Q = -0.235797, R = 0.0006311 from the best fit. The experimental values were then compared with the calculated values obtained using $\sigma = K(p + QE + RE^2)$, where K is the scaling factor. Keeping K as a free parameter and using a χ^2 minimization technique, we obtained K = .79 ± .02 from the best fit. Table 4.6 shows the calculated reaction cross section from the best fit to data at some energies as well as the energy independent σ. Present

results are shown in Fig. 4.1 for the proton interaction loss in NaI along with our calculation using the energy dependent cross section. The calculation using energy independent cross section is hardly distinguishable from the calculation with an energy dependent cross section.

Table 4.6

Reaction cross section values for proton interactions in NaI, as determined from present data

E (MeV)	Energy dependent cross section (mb)	Energy Independent cross section (mb)
151	1274.3	
200	1273.8	
300	1280.1	1273.0
400	1296.3	
500	1322.6	

4.3.2 Deuteron data

In the present experiment, the total interaction loss for 276.8 MeV deuterons in NaI was found to be (39.5 ± 1.7%) as shown in Table 4.7 where the error quoted included both the statistical and the systematic

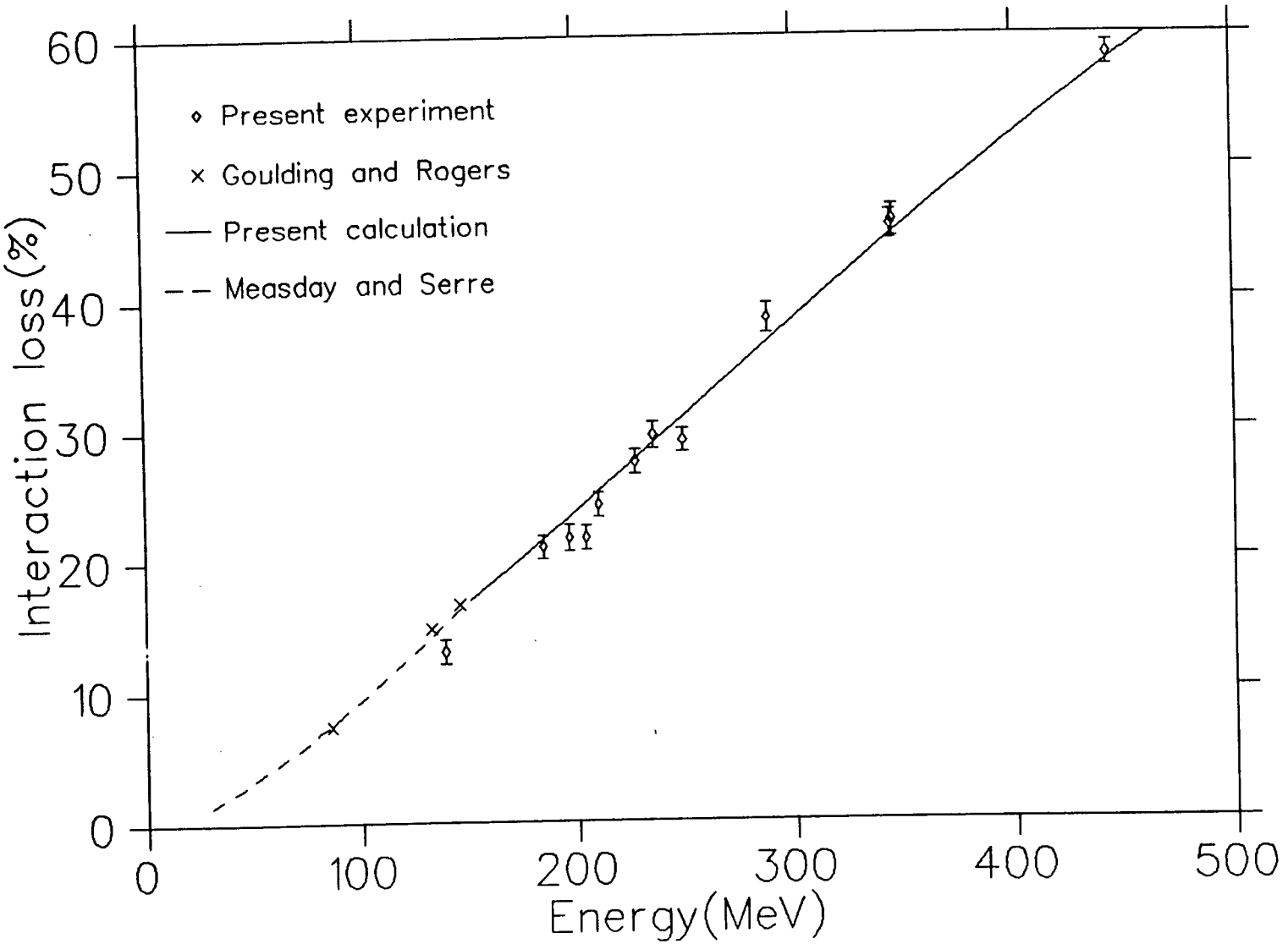

Fig. 4.1: Interaction loss of protons in NaI

Table 4.7

Present result of the deuteron interaction loss

Energy (MeV)	Interaction loss (%)*
276.8	39.5 ± 1.7

* Total error incorporating statistical and systematic.

uncertainties. On the basis of our interaction loss we wanted to calculate the reaction cross section for deuterons in NaI and compare with other results.

The interaction loss for 100 MeV deuterons in NaI as calculated by Measday and Schneider [5] is 9.8%. Taking this value as a reference point, calculations have been done assuming that the 276.8 MeV deuterons lost their energy in NaI til they reached 100 MeV. From the total range of 276.8 MeV deuterons in NaI, the range for 100 MeV deuterons was subtracted and with this range the number of nuclei per cm^2(n) in NaI were calculated. The reaction cross section (σ) for 80 MeV or higher energy deuteron was obtained from the paper [5] as 3520 mb. Based on n and σ, the interaction loss $(1 - e^{-n\sigma})$ for deuteron up to 100 MeV was found. We have included the interaction loss for 100 MeV deuterons as 9.8% of the surviving particles ($9.8\ e^{-n\sigma}$%) and hence the total interaction loss was found to be 47.3%. The interaction loss thus calculated

is somewhat higher than our experimentally measured value. Using our experimental result for the interaction loss, we can compute the effective interaction cross section. The deuteron reaction cross section in NaI for the average deuteron energy of 188.4 MeV ((276.8 + 100)/2) was found to be 2590 ± 180 mb. It is generally known from the theoretical work of Watanabe [33] that in order to explain the angular distributions, polarizations etc, the optical model potential parameters are more or less the same for 94 MeV deuterons and for 45 MeV protons scattered by carbon. This is because each nucleon in the deuteron has half the deuteron energy. This relation apparently works reasonably well at higher energies. Recently N.V. Sen et al., [31,32] studied the elastic scattering of polarized deuterons from ^{16}O, ^{40}Ca and ^{58}Ni at intermediate energies. They [32] mentioned that the total reaction cross section (σ_R = 583 mb) for 400 MeV deuterons in oxygen deduced from the optical model calculations is practically twice the value of σ_R = 295 ± 12 mb, the cross section measured by Renberg et al. [16] for the p - ^{16}O system at 231 MeV. It should be noted here that σ_R should not change much between 200 and 231 MeV since variations of less than 5% were observed beetween 231 and 552 MeV in Renberg's measurement. It was also found from N.V. Sen et al's calculation that the cross section for 700 MeV deuterons, on oxygen is also twice the value measured for 345 MeV protons by Renberg et al. Based on this information it is now generally accepted that the deuteron interaction cross section in matter for deuteron energy E greater than 94 MeV is approximately twice the proton interaction cross section in that matter for protons with energy E/2.

With this empirical relation, we have estimated the reaction cross section of 188.4 deuterons which should be twice the reaction cross section of 94.2 MeV protons in NaI. The reaction cross section thus calculated was found to be 3235 mb. The proton reaction cross section used in this calculation was derived from the existing proton reaction cross section data fitted with an energy dependent quadratic function as mentioned earlier in Section 4.3.1.

In Fig. 4.2, the total reaction cross section for d + ^{16}O are compared to Glauber theory predictions [32]. The microscopic calculations based on Glauber theory are given as a continuous line; data points come from Sen et al's optical model analysis and from the existing results at lower energies, taken from their paper [32]. On the same Figure, we have plotted twice the proton cross section value at half energy as the deuteron cross section at full energy. We can see that above 94 MeV, the deuteron cross section agrees quite well with twice the proton cross section at half the energy.

In Fig. 4.3, the total reaction cross section for d + ^{58}Ni are compared to Glauber theory predictions. The data points and the Glauber theory predictions are taken from Sen et al. [31]. On this figure, as before, we have plotted twice the proton cross section at half energy as the deuteron cross section at full energy. Now, however, the two curves do not agree. Since the proton cross sections for Ni are not known, we have calculated them using values for Fe and making a slight correction by scaling with $A^{2/3}$ (discussed later in this section). The proton cross section data for oxygen and iron were taken from Measday and C. Richard-Serre [1] and Renberg et al. [16].

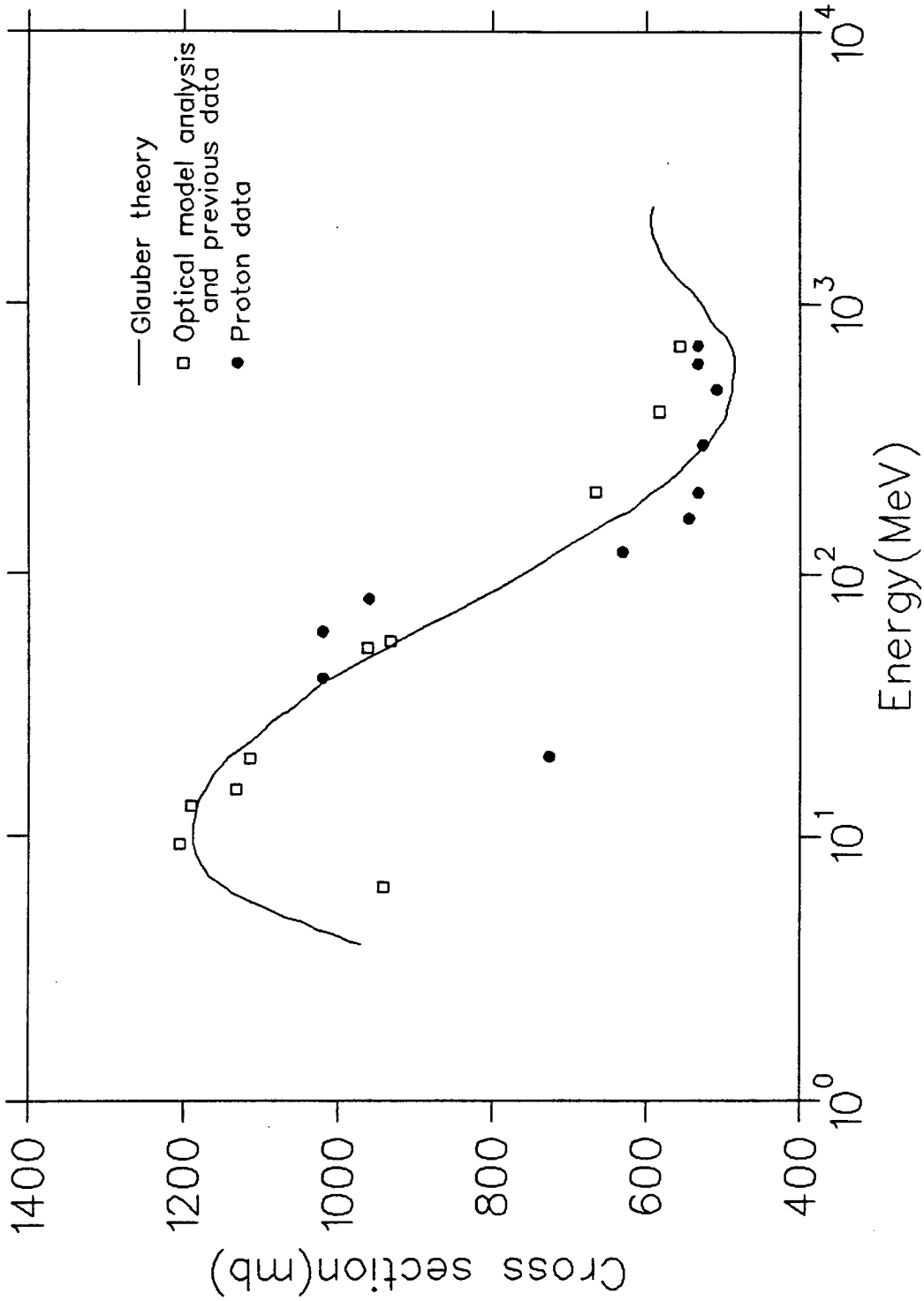

Fig. 4.2: Total reaction cross section for d + ^{16}O along with Glauber theory prediction and previous experimental data as mentioned in Sen et al. [32]

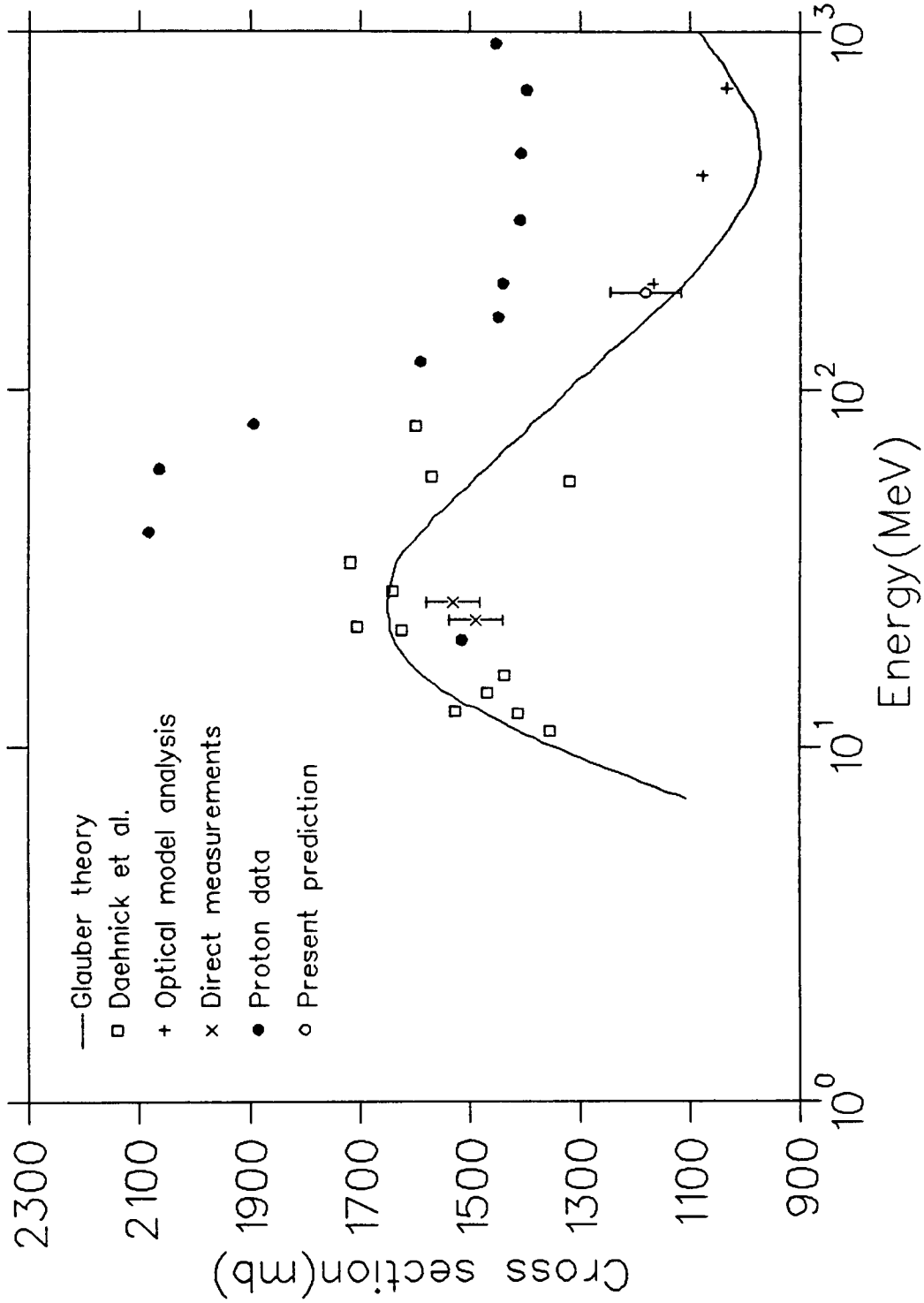

Fig. 4.3: Total reaction cross section for d + ^{58}Ni along with Glauber theory prediction [31] and other results as mentioned in Sen et al. [31]

We finally wanted to predict the reaction cross section for 188.4 Mev deuterons in NaI using extrapolation techniques on the existing deuteron reaction cross section results of oxygen and nickel. The procedure we followed is as follows:

For 230 MeV protons, the reaction cross sections [47] as a function of $A^{2/3}$ were best fitted by

$$\sigma_R = 52.7\ A^{2/3} - 79.1 \tag{4.4}$$

We have selected data at 230 MeV over 550 MeV protons as tabulated [47] assuming that a similar dependence of reaction cross sections on A is true for lower proton energies. Using the above mentioned relation, we could find the relative values of the cross sections for Na and I compared to the cross sections for oxygen and nickel.

$$\begin{aligned} \sigma_{Na} &= 1.360\sigma_O \\ \sigma_I &= 4.90\sigma_O \\ \sigma_{Ni} &= 1.029\sigma_{Fe} \\ \sigma_{Na} &= 0.489\sigma_{Ni} \\ \sigma_I &= 1.761\sigma_{Ni} \end{aligned} \tag{4.5}$$

Using the 188.4 MeV deuteron reaction cross section which is predicted by Glauber theory for oxygen [32] and eq. (4.5), the deuteron reaction cross section in NaI was found to be 3762 mb. Extrapolation of the cross section for high mass iodine on the basis of low mass oxygen may not be very accurate and so the cross section is not very dependable. Using the Gauber theory predicted value of cross section for 188.4 MeV deuteron in nickel [31] and eq. (4.5), the deuteron reaction cross

section in NaI can be obtained as 2529 mb.

Since our experimentally measured interaction loss result for protons were somewhat smaller than the calculated values [1,26] we expected the same for deuterons. Our experimentally measured value of the interaction loss in NaI for the 276.8 MeV deuteron is (39.5 ± 1.7%); from this the 188.4 MeV deuteron reaction cross section was found to be 2590 ± 180 mb; whereas the nickel data based calculation for the 288.4 MeV deuteron cross section in NaI is smaller. This is rather puzzling.

In Fig. 4.4, we have plotted the reaction cross section versus $A^{2/3}$ for 188.4 MeV deuterons. The straight line 1 is drawn using the oxygen and nickel data fron Sen et al. [31,32] and from the extrapolation, the deuteron cross section in NaI is found to be 2318 mb which is quite low and inconsistent with our measurement. The straight line 2 is drawn using the oxygen data [32] and the nickel data calculated from proton reaction cross sections. The deuteron reaction cross section obtained from line 2 is found to be 2990 mb.

We suggest that the reaction cross section for deuterons in nickel, calculated on the basis of proton data, is more dependable than the Glauber theory predictions [31]. Using the reaction cross section for nickel based on proton data, the reaction cross section for 188.4 MeV deuterons was calculated to be 3243 mb. If we extrapolate the cross section in Na using the oxygen data [32], since their masses are close, and the cross section in iodine using the nickel cross section data which was obtained from proton data, the reaction cross section for 188.4 MeV deuterons in NaI was found to be 3356 mb. These two values seem more dependable than the other two extreme values of 2529 mb and

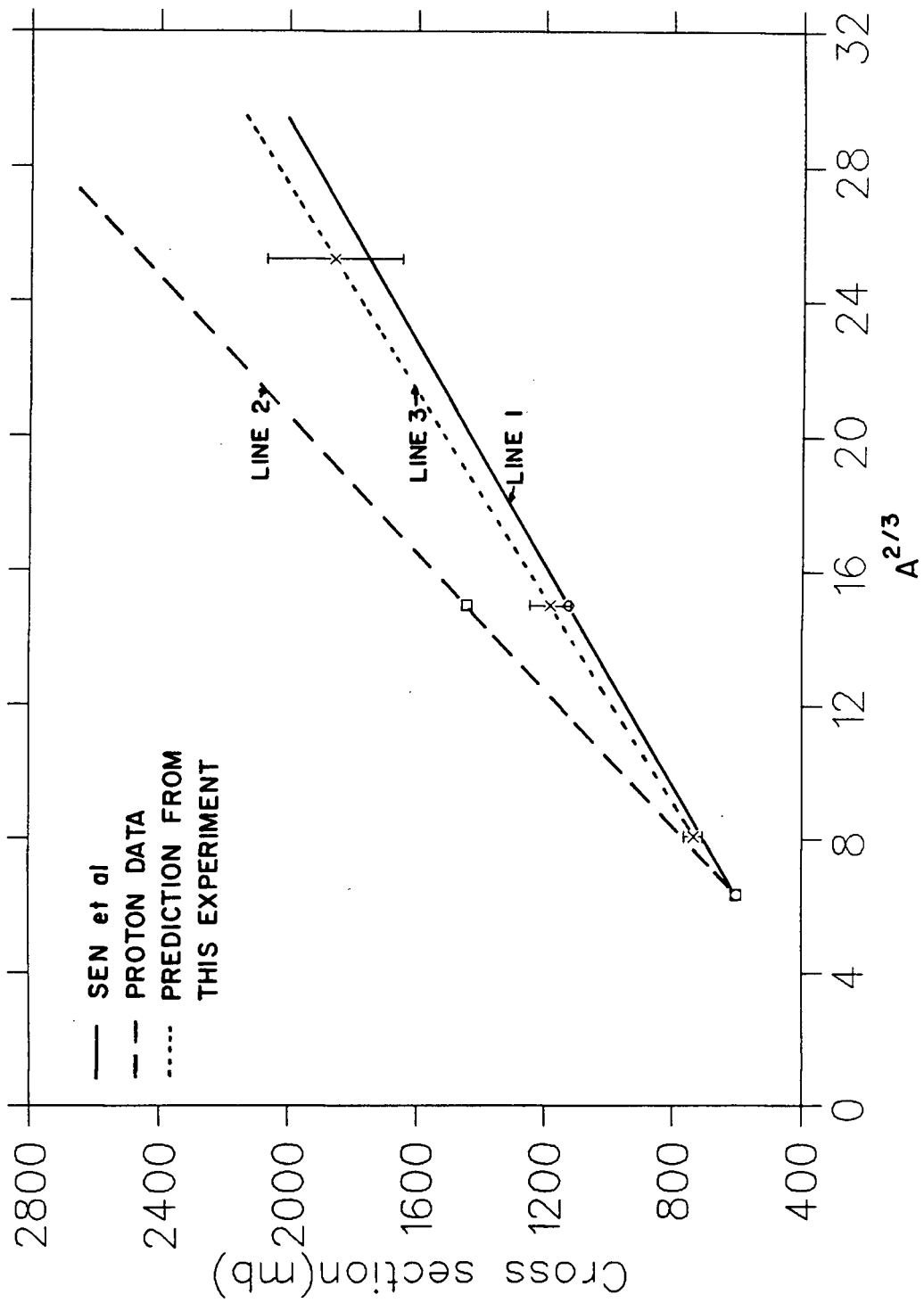

Fig. 4.4: Reaction cross section versus $A^{2/3}$ for 188.4 MeV deuterons

3762 mb.

Again from the empirical relation that σ (d-A) is 2σ (p-A) at half energy, the 188.4 MeV deuteron cross section is found to be 3235 mb, which is twice the 94.2 MeV proton's cross section in NaI found from fit (Section 4.3.1). This value and the one obtained from line 2 (Fig. 4.4), 2990 mb are also dependable values of the reaction cross section for 188.4 MeV deuterons in NaI which are, as expected, a little higher than our effective cross section value, 2590 ± 180 mb obtained from the fit.

Assuming that the reaction cross section in Na is the average of the two values obtained from line 1 and 2, the reaction cross section for iodine was then calculated from the cross section in NaI (σ(NaI) = 2590 ± 180) as obtained from the fit. With these values for Na and I, the third straight line 3 was drawn. The nickel cross section interpolated from line 3 is found to be 1181 mb, which is plotted in Fig. 4.3 at T_d = 188 MeV. We observe that the Glauber theory prediction is even lower, which is puzzling in the light of our proton results.

We thus suggest that the optical model analysis and the Glauber model calculation of Sen et al. both give a slightly low value for the deuteron reaction cross section in the region of a few hundred MeV. We strongly urge physicists to make a direct measurement of this quantity to clarify this very confused situation.

4.4 Summary and conclusions

We have directly measured the reaction losses of protons in NaI detectors for the first time at the relatively high energies of 200-450 MeV. The measurements were done in excellent geometry so that they constitute a measurement of the effective cross section. We have also been able to obtain the interaction loss for deuterons of 277 MeV in NaI.

In the proton measurements the proton beam elastically scattered off a hydrogen target as well as the direct beam was used. For the deuteron measurement a secondary deuteron beam was produced by installing a thin CH_2 target inside the vault section of the cyclotron and the deuterons obtained from the primary proton beam from the $pp \rightarrow d\pi^+$ reaction were transported to the normal target location of the beamline used. We obtain effective reaction cross sections values for protons which are somewhat below direct measurements of this quantity and suggest that some reactions (viz (p, 2p)) can occur, yet the total incident energy is still retained within the crystal.

We have recalculated the losses with an energy dependent cross section $\sigma = P + QX + RX^2$ whose parameters were obtained from the best fit of the recent cross section data. Our experimental data when compared with the calculations were found to be 21% lower. For 276.8 MeV deuterons the reaction losses measured was (39.5 ± 1.7%). Using the interaction loss for 100 MeV deuterons [5] we calculated the loss for 188.4 MeV (average energy) deuteron which was found to be 47.3%. From the fit to our experimental value, the cross section obtained for 188.4

MeV deuteron was 2590 ± 180 mb, which is about 20% lower than the cross section obtained from the empirical relation that σ(d-A) is 2σ(p-A) at half the energy, which is 3235 mb. Our deuteron interaction loss measurement is a very useful result because no other measurement has been made in NaI for intermediate energy deuterons. Furthermore there are few measurements of the deuteron reaction cross sections in this energy range. Most are results of Optical Model analyses or Glauber Model calculations. We show that for deuterons on nickel the recent results of Sen et al. are somewhat low, because our effective cross section lies above their values. The value for nickel was obtained by interpolation and this procedure could be questioned. Nevertheless we feel that the comparison is interesting and indicates that some direct measurements of deuteron reaction cross sections are sorely needed.

Many elastic and quasi-elastic cross section measurements might involve the detection of protons and deuterons in a sodium iodide total energy detector and since it will be used to measure absolute cross sections, it is important to know accurately the efficiency of the detectors for obtaining protons and deuterons in the full energy peak. Since we did not obtain a very good agreement between our experiment and the existing calculated values, we feel further experiments are needed to verify this important effect. We also caution experimenters that there might be some dependence on the size of the NaI crystal. Some calculations with GEANT could be carried out to investigate this interesting possibility.

REFERENCES

1. D.F. Measday and C. Richard-Serre, Nucl. Inst. & Meth., 76 (1969) 45, and CERN report 69-17 (1969).

2. R.A. Giles and E.J. Burge, Nucl. Phys. 50 (1964) 327.

3. M.Q. Makino, C.N. Waddell, and R.M. Eisberg, Nucl. Inst. & Meth., 60 (1968) 109.

4. D.F. Measday, Nucl. Inst. & Meth., 34 (1965) 353.

5. D.F. Measday and R.J. Schneider, Nucl. Inst. & Meth., 42 (1966) 26.

6. K. Bearpark, W.R. Graham, and G. Jones, Nucl. Phys., 73 (1965) 206.

7. E.G. Auld et al., Nucl. Phys., A101 (1967) 65.

8. G.F. Cox et al., Nucl. Phys., B4 (1968) 353.

9. M.R. Wigan et al., Nucl. Phys., A114 (1968) 377.

10. G. Igo, J.C. Fong, and S.L. Verbeck, Nucl. Phys., A195 (1972) 33.

11. R.E. Kozack et al., Ohio State University preprint OSU NSF 355L 1986.

12. M.M. Shapiro, Phys. Rev., 90 (1953) 171.

13. R.E. Pollock and G. Schrank, Phys. Rev., 140B (1965) 575.

14. L.R.B. Elton, Nucl. Phys., 23 (1961) 681.

15. D.V. Bugg et al., Phys. Rev., 146 (1966) 980.

16. P.U. Renberg et al., Nucl. Phys., A183 (1972) 81.

17. C. Serre, CERN Report 67-5 (1967).

18. C.A. Baker et al., Rutherford Laboratory, preprint RPP/P/22 (1969).

19. C. Hojvat and G. Jones, Nucl. Inst. & Meth., 66 (1968) 13.

20. J.J.H. Menet, R.E. Gross, J.J. Malanify, and Z. Zucker, Phys. Rev. Lett. 22 (1969) 1128.

21. J.F. Dicello and G. Igo, Phys. Rev., C2 (1970) 488.

22. L.H. Johnston et al., IRE Trans. Nucl. Sci., NS-5 (1958) 95.

23. A. Johansson, U. Svanberg, and O. Sundberg, Ark. Fys. 19 (1961) 527.

24. J.N. Palmieri and J. Wolfe, Nucl. Inst. & Meth., 76 (1969) 55.

25. A.M. Sourkes et al., Nucl. Inst. & Meth., 143 (1977) 589.

26. G.A. Goulding and J.G. Rogers, Nucl. Inst. & Meth., 153 (1978) 511.

27. J.M. Cameron et al., Nucl. Inst. & Meth., 143 (1977) 399.

28. A. Bracco et al., Nucl. Inst. & Meth., in Phy. Res. 219 (1984) 329.

29. J. Bojowald et al., Annual Report of Institut fur Kernphysik, Julich, (1986) p 6.

30. R. Eisberg, Nucl. Inst. & Meth., 146 (1977) 487.

31. N.V. Sen et al., Phys. Lett., 156B (1985) 185.

32. N.V. Sen et al., Nucl. Phys., A464 (1987) 717.

33. S. Watanabe, Nucl. Phys., 8 (1958) 484.

34. J. Spuller et al., Phys. Lett. 67B (1977) 479.

35. R. MacDonald et al., Phys. Rev. Lett., 38 (1977) 746.

36. V.L. Highland et al., Nucl. Phys., A365 (1981) 333.

37. E. Mazzucato et al., Phys. Rev. Lett., 96B (1980) 43.

38. B. Bassalleck et al., Nucl. Phys., A362 (1981) 445.

39. K.A. Aniol et al., Phys. Rev., A28 (1983) 2684.

40. P. Depommier et al., Phys. Rev. Lett., 39 (1977) 1113.

41. D. Bryman, P. Depommier and C. Leroy, Phys. Reports 88 (1982) 151.

42. D.A. Bryman et al., Phys. Rev. Lett., 50 (1983) 7.

43. D.A. Bryman et al., Phys. Rev. Lett., 50 (1983) 1546.

44. G. Azuelos et al., Phys. Rev. Lett., 51 (1983) 164.

45. C.E. Picciotto et al., Phys. Rev. D., 37 (1988) 1131.

46. M. Hugi et al., Nucl. Phys., A472 (1987) 701.

47. D.F. Measday, M.R. Menard, J.E. Spuller, TRIUMF Kinematics Handbook (edition 1).

48. J.F. Bartlett et al.; Fermilab multicomputer program for data acquisition and analysis, 1981. TRIUMF implementation by Y. Miles.

49. Anne W. Bennett. A command language programme: MOLLI (1983). [MOLLI is a command language program that reads data written with the TRIUMF data acquisition program (MULTI) initially written in April 1983 by A. Bennett and revised by J. Lloyd].